nature communications

Article

https://doi.org/10.1038/s41467-025-60057-0

Divergent antibody recognition profiles are generated by protective mRNA vaccines against Marburg and Ravn viruses

Received: 12 March 2024

Accepted: 13 May 2025

Published online: 01 July 2025

Check for updates

Michelle Meyer[1,2], Bronwyn M. Gunn[3], Colette Pietzsch[1,2], Chandru Subramani[1,2], Kritika Kedarinath[1,2], Paula P. Villarreal[4], Matthew A. Hyde[2], Erica Ollmann Saphire[5], James E. Crowe Jr.[6,7,8], Galit Alter[9], Sunny Himansu[10], Andrea Carfi[10] ✉ & Alexander Bukreyev[1,2,11,12] ✉

The first-ever recent Marburg virus (MARV) outbreak in Tanzania and recent emergences in Rwanda, Ghana and Equatorial Guinea underscore the importance of therapeutic or vaccine development against the virus, for which none are approved. mRNA vaccines were proven successful in a pandemic-response to severe acute respiratory syndrome coronavirus-2, making it an appealing platform to target pathogenic emerging viruses. Here, we develop 1-methyl-pseudouridine-modified mRNA vaccines formulated in lipid nanoparticles (LNP) targeting the glycoproteins (GP) of MARV and the closely-related Ravn virus (RAVV). Vaccination of female guinea pigs elicits robust binding and neutralizing antibodies and confers complete protection against homologous and heterologous virus replication, disease and death. Characterization of antibody responses identifies disparities in the binding and functional profiles between the two viruses and regions in GP that are broadly reactive. The glycan cap is highlighted as an immunoreactive site for orthomarburgviruses, inducing antibody responses that are virus dependent. Profiling the antibody responses against the two viruses provides insight into how antigenic differences may affect the response towards conserved GP regions, which would otherwise be predicted to be cross-reactive, and has implications for the future design of broadly protective vaccines. The results support the use of mRNA-LNPs against pathogens of high consequence.

Marburg virus (MARV) and Ravn virus (RAVV) cause a severe disease in humans. The viruses belong to the genus *Orthomarburgvirus*, within the *Filoviridae* family. The family also includes the genus *Orthoebolavirus* with members such as Ebola virus (EBOV) and Sudan virus (SUDV). Given the recent concurrent MARV outbreaks in two non-endemic countries of Africa, Equatorial Guinea[1] and the United Republic of Tanzania[2], and a 24–88% case fatality rate[3], the perceived risk of MARV spreading similarly to the unprecedented 2013–2016 West-African EBOV outbreak is justified. There are currently no licensed vaccines against MARV; however, several vaccine constructs have demonstrated protective efficacy in non-human primates (NHPs)[4–9]. Advances have been made across multiple vaccine platforms that rely on virus glycoprotein (GP) antigens to induce protective immune responses. Some of these candidates have shown promise in Phase I clinical trials or are on the cusp of entering trials. However, these candidates need to be assessed during an outbreak setting.

A full list of affiliations appears at the end of the paper. ✉e-mail: andrea.carfi@modernatx.com; alexander.bukreyev@utmb.edu

Virus-vectored vaccines have been tailored against MARV, with some based on constructs previously validated in clinical trials for the closely related EBOV. Two vesicular stomatitis virus (VSV)-derived vaccines against MARV variants Angola and Musoke, similar to the fully-licensed EBOV vaccine, Live (tradename: ERVEBO; Merck Sharp & Dohme), were efficacious in preclinical studies[10,11], and a Phase I safety and immunogenicity trial of the Angola vaccine in healthy adults has commenced. Efforts are underway to reduce the vaccine-associated side-effects by implementing a further attenuated version of the platform[12].

Heterologous prime-boost combinations of replication-incompetent multivalent adenovirus type 26 (Ad26)- and Ad35-based MARV vaccines, engineered similarly to the Ad26 component used in the approved Johnson & Johnson (J&J) Janssen heterologous prime-boost EBOV vaccine regimen (Ad26.ZEBOV-GP [recombinant], Zabdeno, with MVA-BN-Filo [recombinant], Mvabea), protected 75–100% of MARV-infected NHPs[5]. Phase II clinical trials of a recombinant adenovirus vaccine based on chimpanzee adenovirus 3, which mitigates vector immunity, are underway in Africa, after successful demonstration of safty and long-term antibody responses in adults in the USA[13] and rapid and durable efficacy in NHPs[7]. Capitalizing on the Oxford-AstraZeneca Coronavirus Disease 2019 (COVID-19) platform, a ChAdOx1 chimpanzee adenovirus vaccine entered Phase I trials. However, small animal models could not demonstrate reliable efficacy against MARV challenge[14,15], and no NHP challenge data are currently available.

The Mvabea constituent of the Janssen vaccine is a modified vaccinia Ankara viral vector expressing antigens from four different filoviruses, including the GP from MARV variant Musoke (93% amino acid homology to Angola GP), but its efficacy against MARV was never fully assessed[16,17]. DNA-based vaccines yielded limited seroconversion in Phase I clinical trials despite multiple boosters[18]. Virus-like or inactivated virus particles require multiple, adjuvanted doses to confer NHPs with protection against MARV and heterologous RAVV[4,6].

We have previously shown that a two-dose regimen of a modified mRNA vaccine encoding EBOV GP, formulated with a lipid encapsulation, effectively protected guinea pigs against EBOV[19]. Our results provided evidence that the mRNA platform could be a formidable vaccine against pathogens of high consequence. The need remains for vaccine platforms that target other closely related members of the *Filoviridae* family, given that the current licensed vaccines are virus vector-based and shown to be efficacious against EBOV only, in clinical settings.

Eliminating virus vector backbones as the delivery vehicle for encoded antigens has advantages. Vector-less delivery provides the capacity to design a more targeted response without complications from vector-generated adverse effects. Issues of preexisting immunity toward the vector delivery vehicle are also circumvented allowing for repeat dosing and a reimagined vaccine platform against a spectrum of pathogens.

Ever since protein expression from exogenously introduced naked mRNA was demonstrated in mouse muscle[20], the development of mRNA as vaccines against infectious diseases has gained steady momentum. mRNA vaccines were modified to bypass the body's immune defenses and encapsulated by lipid nanoparticles (LNP) to facilitate delivery. While mRNA vaccines targeting viruses including influenza virus, respiratory syncytial virus, and Zika virus, advanced through Phase I and II trials[21–23], it will be years before they are clinically accessible. The full potential of mRNA vaccines was realized at the onset of the COVID-19 pandemic, which propelled regulatory approval and widespread administration of what at the time was still considered a novel platform[24].

In this study, we assess the effectiveness of mRNA vaccines encoding the GP from two closely-related, but genetically distinct orthomarburgviruses, MARV and RAVV, by testing the efficacy of a two-dose regimen against the respective viruses in the guinea pig model. GP is structurally similar among filoviruses, comprised of two subunits, GP1 and GP2, held together in a trimeric conformation resembling a challis. The receptor binding domain (RBD), glycan cap (GC) and mucin-like domain (MLD) are found within GP1. GP2 contains a wing domain unique to orthomarburgviruses, a fusion loop, and heptad repeat structures that anchors GP at the C-terminal end. While the domains of GP facilitate key viral functions, they may also fashion the functional properties of antibodies, with the epitopes for neutralizing antibodies located in the RBD[25] and antibodies which block virus egress located in MLD[26]. The wing domain was identified as the site for antibodies which mediate immune cells through their Fc-effector functions[27]. Despite the structural similarities among the GPs of filoviruses, only 30% of the amino acid sequence is identical between MARV and EBOV, and occurs primarily in the RBD and GP2[28]. Cross-protection against both MARV (variant Angola) and RAVV is of concern given that their GPs are 22% divergent at the amino acid level[29] with high incongruity found in the MLD or GC regions, each possessing an identity of approximately 50%. We designed mRNA sequences from two distantly related orthomarburgviruses to mitigate the risk of susceptibility to heterologous virus challenge. However, we show that our mRNA vaccines protect against both homologous and heterologous virus challenges. In addition to survival analysis, we characterize the functional properties of the antibody response and map targeted antigenic sites to reveal the commonalities and uniqueness between the MARV and RAVV mRNA vaccine-induced profiles. Our results further support the advancement of the mRNA vaccine platform development against highly lethal viruses.

Results

mRNA design, generation, and vaccination schedule

mRNA vaccines encoding the GP of MARV or RAVV were synthesized in vitro from linearized DNA templates by T7 polymerase-mediated transcription in which the uridine-triphosphate (UTP) was substituted with 1-methylpseudo-UTP. mRNA constructs were then encapsulated in LNP formulations for subsequent delivery in vivo as previously described[30]. Two groups of Hartley guinea pigs ($n = 5$ per group) were vaccinated via the intramuscular route with the MARV or RAVV mRNA-LNP vaccine, receiving a prime dose on day 0 and a booster dose on day 27 (Fig. 1). Two control groups of guinea pigs ($n = 5$ per group) were mock vaccinated with phosphate buffered saline (PBS). Over the vaccination phase of the study, serum was collected, and the antibody binding and functional profiles were characterized.

Both mRNA vaccines generate autologous and asymmetric heterologous virus-neutralizing antibody responses

Following each vaccination dose, we monitored virus-specific antibody responses in serum. High anti-MARV or -RAVV IgG titers were detected by enzyme-linked immunosorbent assays (ELISA) 27 days after the prime dose of the respective mRNA vaccine (Fig. 2A), which was further elevated by the booster dose. MARV- and RAVV-specific IgG titers were comparable after both the prime and boost vaccinations. Both vaccines also induced neutralizing antibodies against their respective viruses, which somewhat mirrored the IgG response in that titers measured after prime vaccination were further elevated by the booster (Fig. 2B).

Given that MARV and RAVV are genetically distinct but share 78% GP sequence identity at the amino acid level, we determined the ability of the serum collected after the boost vaccination to neutralize heterologous virus (Fig. 2C). The MARV vaccine autologous virus-neutralizing antibody titer was lower compared to the autologous virus-neutralizing titer generated by the RAVV vaccine (Fig. 2B). However, the MARV vaccine induced a higher cross-neutralizing titer against RAVV (reciprocal neutralizing titer 50 [NT_{50}] of 89.0) compared to the RAVV vaccine neutralizing titer against MARV (NT_{50} of 8.2) (Fig. 2C).

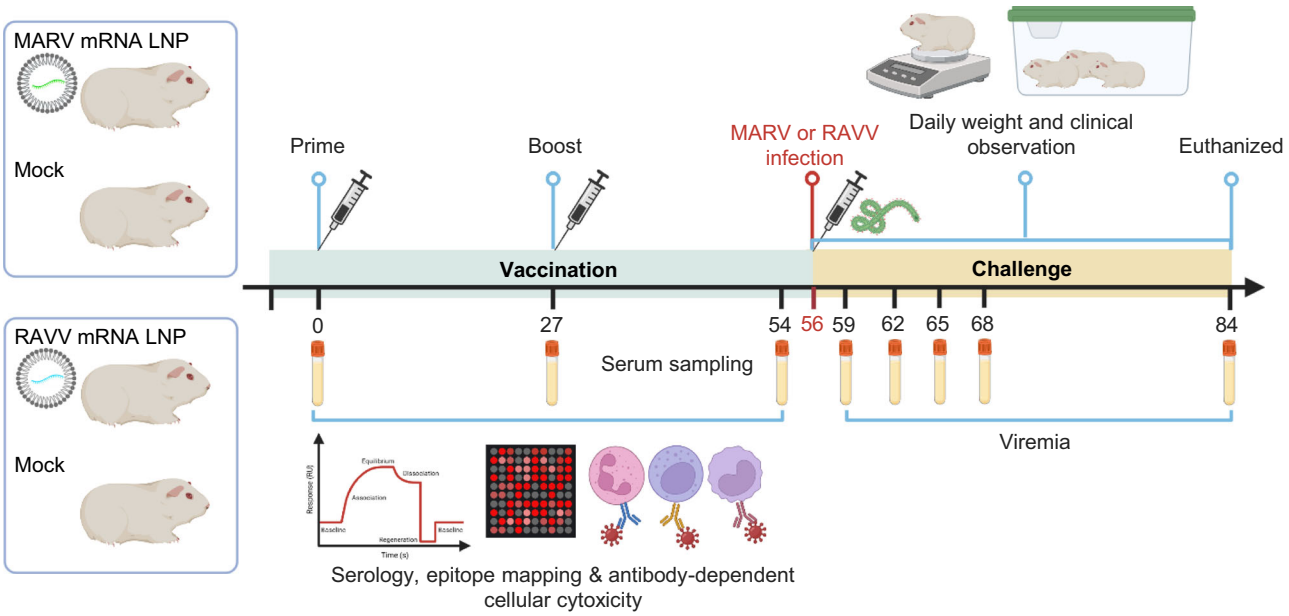

Fig. 1 | Schematic of mRNA vaccine challenge study design. Guinea pigs were vaccinated ($n = 5$ per vaccine) via the intramuscular route on day 0 and boosted on day 27 with MARV mRNA (green) or RAVV mRNA (blue). Control groups were mock vaccinated ($n = 5$ per virus). Animals were challenged with 1000 plaque-forming units (PFU) of guinea pig-adapted MARV or RAVV by the intraperitoneal route at day 56. All animals were monitored for changes in weight, clinical scores, and survival over 28 days. Serum was collected from each animal over the course of infection and measured for infectious virus. Created in BioRender. Meyer, M. (2025) https://BioRender.com/8a2gmvi.

These data demonstrate that MARV and RAVV mRNA vaccines elicit comparable binding antibody responses after prime and boost doses against their respective viruses. The RAVV vaccine yielded higher autologous neutralizing antibodies than MARV, but the MARV vaccine appeared to induce a more cross-neutralizing response.

The mRNA vaccines differ in their response towards the proteolytically cleaved form of GP

We further assessed the level of homologous binding to truncated forms of GP (Fig. 3A): MARV or RAVV GP ectodomains (GPΔTM), mucin-deleted ectodomains (GPΔmuc, Δ257–425), proteolytically-cleaved GPs (GPcl), and the wing-deleted RAVV GPΔmuc (GPΔmucΔw, additional deletion of residues Δ436-483). All GP forms were immobilized on Octet biolayer interferometry (BLI) sensors at comparable levels and allowed to bind antibodies in serum. In general, similar levels of antibody binding were observed between MARV- and RAVV-vaccine-derived sera to immobilized GPΔTM or GPΔmuc from the respective virus (Fig. 3B). MARV-specific serum antibodies appeared to have a lower binding capacity to GPcl than RAVV-specific serum antibodies. Therefore, the response generated from MARV mRNA vaccination may target the GC, which is absent on the proteolytically cleaved form of GP, more so than RAVV vaccination.

The MARV vaccine induces a greater antibody response to the GP glycan cap compared to the RAVV vaccine

The proportion of the vaccine-induced antibody response directed toward regions on MARV or RAVV GP [MLD, GC or RBD of the GP1 subunit, and the wing and base regions of the GP2 subunit] was determined to identify the regions predominantly responsible for the binding antibody response to vaccination. GP region-specific responses were measured using BLI competition assays (Fig. 3C). Serum antibodies from vaccinated animals were allowed to bind to a GP immobilized on the BLI sensor after pre-adsorption with a GP variant (Fig. 3A) which removed antibodies targeting regions shared between the competing and immobilized GPs. The proportion of MLD-specific antibodies was inferred from the percentage of serum antibody binding to GPΔTM not removed by GPΔmuc pre-adsorption (Fig. 3D). MLD antibodies in MARV vaccine recipients comprised approximately 40% of the response (Fig. 3E). The proportion of MLD antibodies in RAVV vaccine recipients was similar to that of MARV recipients. GPcl, the protease cleaved form of GP, lacks GC which is present in GPΔmuc and GPΔTM. We could therefore deduce the proportion of antibodies binding to the GC; the level of binding to GPΔTM inhibited by GPcl pre-adsorption was subtracted from the level of binding to GPΔTM inhibited by GPΔmuc pre-adsorption (Fig. 3D, E). Approximately 55% of the MARV-directed response towards GPΔTM targeted the GC (Fig. 3E). However, the proportion of GC-targeted antibodies in the RAVV vaccine response (~17%) was substantially lower than in the MARV vaccine response. The proportion of GC antibodies could also be calculated using other combinations of competing truncated GP proteins (Fig. 3E): (i) the level of binding to GPΔmuc inhibited by GPcl pre-adsorption subtracted from the level of binding to GPΔmuc inhibited by GPΔTM pre-adsorption, or (ii) the level of binding to GPΔmuc not inhibited by GPcl pre-adsorption. When GPΔmuc was used as the capture ligand instead of GPΔTM (Fig. 3D), GC antibody proportions were augmented to approximately 70% for the MARV response and 30% for the RAVV response (Fig. 3E), given the relative surface area of GC to GPΔmuc is greater than its relative surface area to GPΔTM.

The fraction of the response towards the combined RBD, wing and GP2 regions was determined by the level of binding to GPΔTM or GPΔmuc inhibited by the presence of GPcl (Fig. 3D, E). The MARV-vaccine response towards this combined region was 30% less than the RAVV response. The greater proportion of GC antibodies relative to the total amount of binding antibodies in MARV vaccine recipients may have offset the response towards the combined RBD, wing and GP2 regions. However, the higher frequency of RAVV antibodies towards the combined RBD, wing and GP2 regions was confirmed using the reverse setting, which measured the level of binding to GPcl inhibited by GPΔmuc or GPΔTM pre-adsorption.

The proportion of the response directed to the wing domain could only be determined for RAVV due to the availability of RAVV-derived GPΔmucΔw. The level of serum binding to GPΔmuc following

https://doi.org/10.1038/s41467-025-60057-0

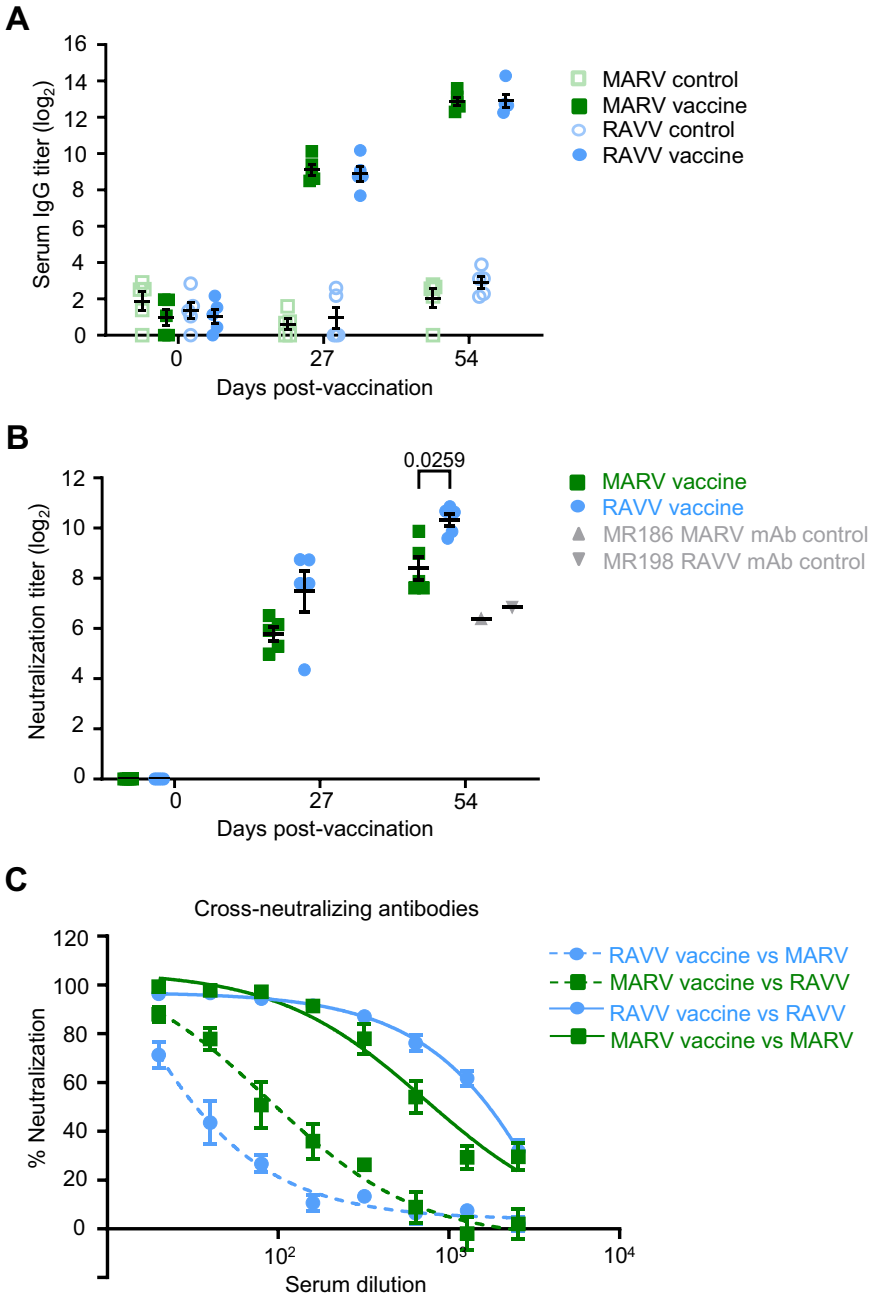

Fig. 2 | Serum antibody responses are produced in MARV and RAVV mRNA vaccinated guinea pigs. A Serum GP-specific IgG and (**B**) virus-neutralizing antibody titers against homologous or (**C**) heterologous viruses targeted by the vaccines were measured using ELISA or plaque reduction neutralization assays, respectively. Antibody titers in (**A**–**C**) MARV ($n = 5$, solid square), RAVV ($n = 5$, solid circle) and (**A**) control ($n = 5$ per virus; square outline, MARV and circle outline, RAVV) vaccinated groups prior to MARV (green) or RAVV (blue) infection. Bars denote group means ± SEM. **B** Antibody titers required to achieve 60% virus neutralization. Known neutralizing mAbs, MR186 (gray triangle) and MR196 (gray inverted triangle), included as assay controls. **C** Virus-neutralizing antibody dilution curves for day 54 serum against homologous (solid lines) or heterologous viruses (dashed lines). **A**, **B** Only significance between MARV and RAVV vaccine recipients, measured by repeated measures two-way ANOVA with Sidak's correction for multiple comparisons, is shown.

pre-adsorption with GPΔmucΔw was used to calculate the frequency of the response towards the wing domain. Interestingly, GPΔmucΔw had minimal effect on blocking antibody binding to all GP forms in the competition assays indicating that most of the response targeted the wing domain (supplementary Fig. 1A). However, in the reverse setting, preadsorption with the truncated GP forms prevented a substantial portion of serum binding to immobilized GPΔmucΔw (supplementary Fig. 1B). Therefore, the actual wing domain antibody proportions in serum antibodies may be misrepresented in this assay system. The total response binding to GPΔmucΔw was poor (supplementary Fig. 1C). Furthermore, binding to the wing domain facilitates the structural rearrangement of GP to enhance binding of RBD antibodies[27]. The absence of the wing domain in GPΔmucΔw may have prevented the sequesteration of serum RBD antibodies by thwarting the cooperative recognition of RBD that occurs upon engagement of the wing domain. During preadsorption with GPcl, approximately 60% of serum antibodies were sequestered by the RBD and GP2 regions, thereby preventing subsequent binding to GPΔmucΔw (supplementary Fig. 1B). This indicates that 40% of the antibodies were reactive with GC (consistent with GC proportions calculated in Fig. 3E).

Overall, these data demonstrate that both vaccines comparably target the MLD, but the MARV vaccine induces a greater antibody

https://doi.org/10.1038/s41467-025-60057-0

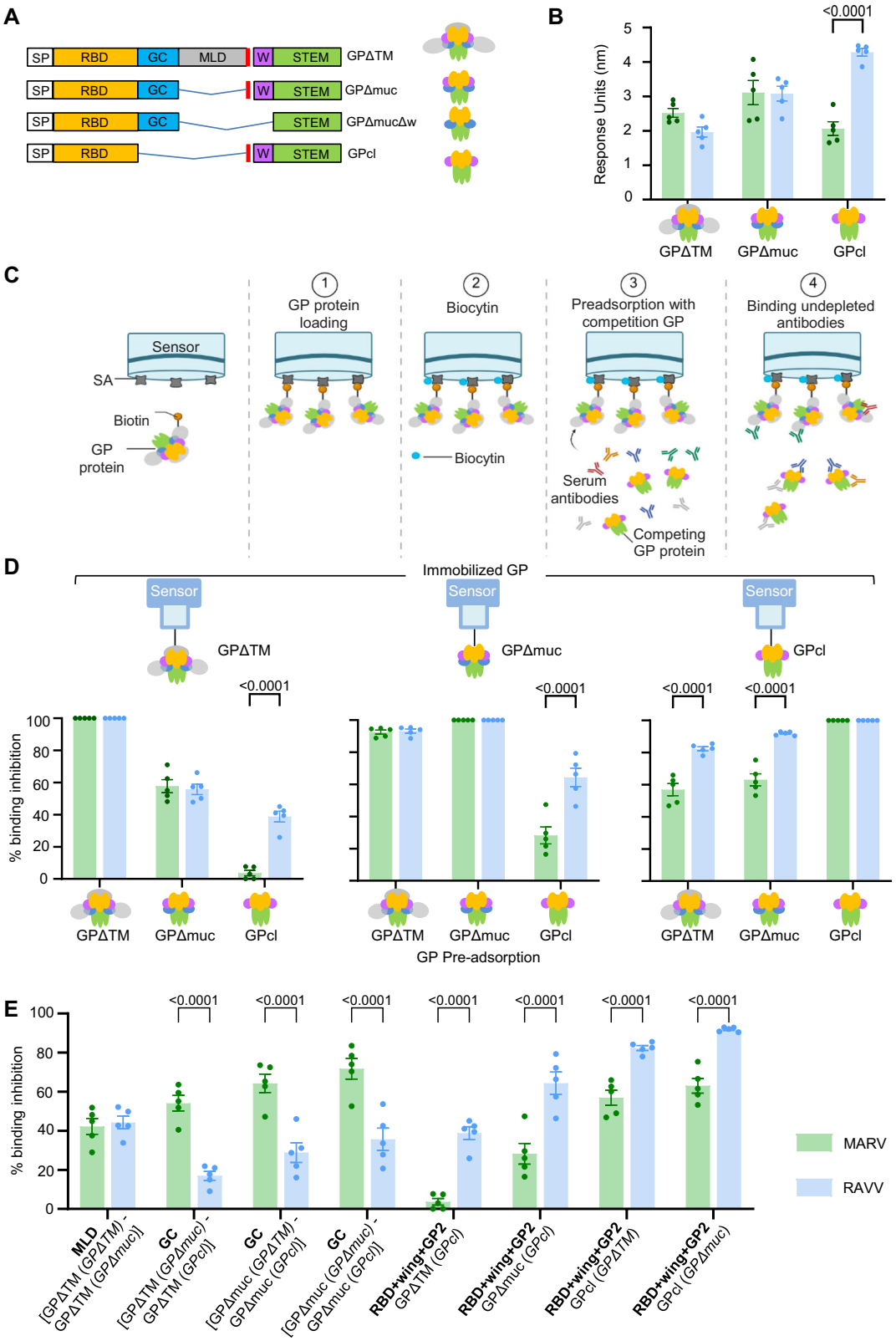

response to GC, while the RAVV vaccine induces a greater response toward the combined RBD, wing and GP2 regions.

MARV and RAVV vaccines induce virus-neutralizing antibodies specific for different regions of GP

We next determined the regions on GP targeted by neutralizing antibody responses generated by the MARV or RAVV mRNA vaccines. Day 54 sera from MARV- or RAVV-vaccinated guinea pigs were diluted to a concentration required to achieve at least 80% virus neutralizing activity. Diluted sera were then pre-absorbed with increasing concentrations of truncated GP proteins derived from the respective vaccine-targeted viruses (MARV GPΔmuc and GPcl or RAVV GPΔmuc, GPΔmucΔw and GPcl). The presence of the truncated GP proteins sequestered antibodies that bound to regions shared with the full-length GP on the virus.

Fig. 3 | MARV and RAVV vaccines generate different proportions of binding antibodies targeting GP regions. A Schematic of truncated GP forms. Blue lines represent deleted regions. SP, signal peptide (white); RBD, receptor binding domain (gold); GC, glycan cap (blue); MLD, mucin-like domain (gray); W, wing (purple); STEM, GP2 lacking the transmembrane domain (TM, green). GPΔTM GP ectodomain, GPΔmuc GP mucin-deleted ectodomains, GPcl proteolytically-cleaved GP, GPΔmucΔw wing-deleted RAVV GPΔmuc. Red line indicates the furin cleavage site. **B**, **D**, **E** Day 54 MARV (green) and RAVV (blue) post vaccination serum ($n = 5$ per group) (**B**) binding to truncated GP forms depicted as response units. **C** Schematic of GP competition assay. Biotin labeled GP is immobilized on a streptavidin sensor. A streptavidin sensor is treated with biocytin and dipped in a solution containing serum preabsorbed by the competing GP. Serum antibodies which are not depleted by the competing GP bind to the GP immobilized on the sensor. Created in BioRender. Meyer, M. (2025) https://BioRender.com/w6beb8i. **D** Binding inhibition to immobilized GPΔTM, GPΔmuc or GPcl expressed as a percentage of total binding response unit values obtained without serum pre-adsorption. **E** Proportion of the antibody response binding to the MLD, GC and combined RBD, wing and GP2 regions. The mean responses of each group are shown as bars, with ± SEM. Significance between MARV and RAVV vaccine recipients measured by two-way ANOVA with (**A**, **C**) Sidak's or (**E**) Holm-Sidak's correction for multiple comparisons.

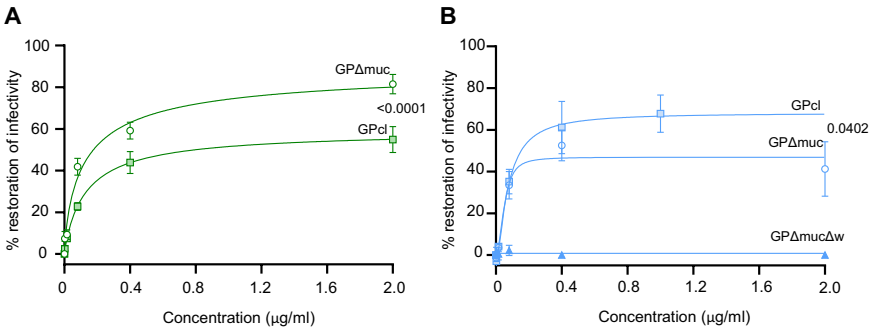

Fig. 4 | The epitope specificity of neutralizing antibodies from MARV and RAVV mRNA vaccine recipients differ. Neutralizing activity of day 54 (**A**) MARV (green) or (**B**) RAVV (blue) mRNA vaccine immune sera ($n = 5$ per vaccine) pre-absorbed with GPΔmuc (circle outline) and GPcl (solid square) or GPΔmucΔw (solid triangle, RAVV only) expressed as a percentage relative to the neutralizing activity of the same sera without pre-adsorption. Sera from MARV or RAVV vaccinated groups, diluted to achieve 80% of their neutralization activity, were incubated with increasing concentrations of truncated GPs from the relevant virus. The percentage of restoration of infectivity is plotted against concentration of competing GP. Data points denote group means ± SEM. Curves were fit using the least-squares fit method of non-linear regression analysis. Extra sum-of-squares F test was performed to determine significant differences in best-fit parameters between GPΔmuc and GPcl curves: (**A**) $p < 0.0001$; $F(4,52) = 11.45$ (**B**), $p = 0.0402$; $F(4,62) = 2.671$.

The ability of serum from MARV mRNA-vaccinated animals to neutralize the virus was nearly abolished with increasing concentrations of MARV GPΔmuc, indicating that non-MLD-specific antibodies are major contributors to the neutralizing capacity of serum antibodies (Fig. 4A). The ability of non-MLD antibodies to neutralize virus in the presence of MARV GPcl was diminished to a lesser extent compared to neutralization in the presence of MARV GPΔmuc, indicating that antibodies targeting the GC structure, absent in MARV GPcl, contribute to virus neutralization.

For RAVV-vaccinated animals, non-MLD-binding antibodies also contributed to neutralization activity, although seemingly to a lesser extent than the MARV-derived antibodies since infectivity was not fully restored in the presence of RAVV GPΔmuc (Fig. 4B). While this finding may suggest that a substantial proportion of the RAVV-vaccine derived neutralizing antibodies targets the MLD, the presence of increasing concentrations of GPcl, the furin cleaved form of GP which lacks both the GC and MLD domains, restored virus infectivity to a better extent than GPΔmuc. Accessibility to the RBD on the cleaved structure may enable improved sequestering of RBD-specific neutralizing antibodies. This finding also indicates that RAVV vaccine-derived neutralizing antibodies targeted GP in its cleaved form better than the MARV vaccine-derived neutralizing antibody response.

Interestingly, RAVV virus infectivity was not restored in the presence of GPΔmucΔw, indicating that the RAVV wing domain is important for neutralization activity. Taken together, these data demonstrate that the GP regions targeted by neutralizing antibodies diverge between the two vaccines: the GC region was heavily involved in the neutralization response after MARV vaccination, while the RBD, wing and GP2 regions of the GPcl structure contributed substantially to the neutralization response following RAVV vaccination.

The vaccines induce antibodies binding to protective epitopes in RBD and wing domain

We quantified the prevalence of the response directed to known protective epitopes in the RBD and wing domain of GP. Representative monoclonal antibodies (mAbs) isolated in our previous studies from human survivors with epitopes in the RBD (MR72, MR78, MR82, MR111, MR191 and MR198), and the wing domain (MR228 and MR235)[25,27] were selected to compete for binding to GP on the BLI platform with serum antibodies collected after the booster dose (supplementary Fig. 2). MR111 binds to RAVV GP but not MARV GP, and all RBD-specific mAbs are neutralizing antibodies[25]. The two mAbs specific to the wing domain do not neutralize virus but have Fc-mediated effector functions[27]. MR228 binds the wing domain of MARV GP, but not RAVV GP, limiting the number of wing domain antibodies that could be used to compete for RAVV GP binding. Among these antibodies, MR72, MR78, MR82 and MR228 protected small animal models[25,27,31], while MR191 protected NHPs[31]. Serum from recipients of the MARV mRNA vaccine showed comparable levels of reactivity towards all representative RBD epitopes (Fig. 5A). The response towards all RBD mAb epitopes, except for MR72, was lower in frequency than the response towards the wing domain epitope for MR228. The antibody frequency towards the wing domain epitope for MR235 was comparable to the RBD-targeted response. Conversely, the frequency of antibodies from RAVV mRNA recipients was similar towards most RBD epitopes, except the epitopes for MR82 and MR198. The frequency of antibodies targeting RBD epitopes was generally higher than the frequency directed towards the wing domain epitope for MR235 (Fig. 5B). Overall, the response recognition frequency to known epitopes in the RBD and wing domains appeared to differ between the MARV and RAVV mRNA vaccines.

https://doi.org/10.1038/s41467-025-60057-0

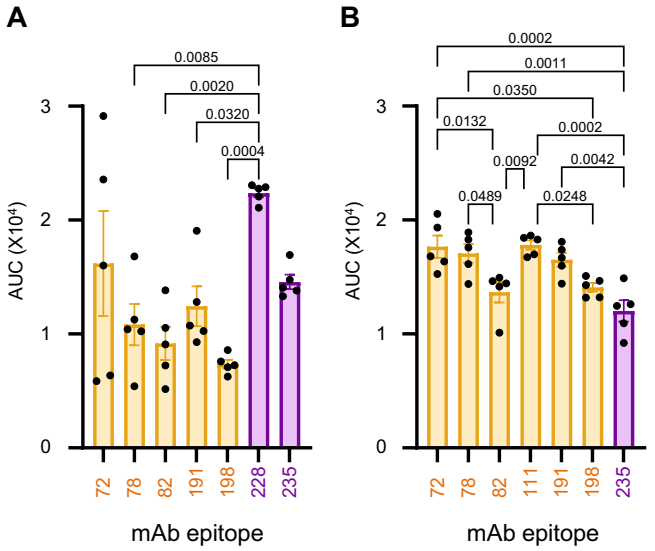

Fig. 5 | The prevalence of immune sera targeting known epitopes of human survivor mAbs are different between MARV and RAVV mRNA recipients. BLI-based competition-binding assay in which mAbs compete with day 54 pre-infection serum antibodies from (**A**) MARV ($n = 5$) or (**B**) RAVV ($n = 5$) vaccine recipients for a specific epitope on biotinylated (**A**) MARV or (**B**) RAVV GPs immobilized on streptavidin sensors. The level of inhibition was determined as a percentage of blocking activity relative to mock-control sera against the tested mAb. Area under the curve (AUC) of normalized binding inhibition values calculated from a dilution series of each serum sample. Symbols indicate individual guinea pigs. Bars denote the average blocking of RBD mAbs (gold) or wing domain mAbs (purple) by sera from vaccinated groups ± SEM. Significance measured by one-way ANOVA with Tukey's correction for multiple comparisons between the serum prevalence towards different mAb epitopes.

The vaccines induce antibodies specific for both cross-reactive and unique linear epitopes

The MARV and RAVV vaccine antibody response profiles were further scrutinized for any parallels or uniqueness in their linear epitope recognition patterns. Linear epitopes of GP targeted by antibodies were characterized using peptide arrays designed with overlapping 15-mer peptides spanning the entire GP of MARV (variant Angola) or RAVV, offset by 4 amino acids. Serum antibodies in samples collected after boost vaccination dose were allowed to bind each of the GP arrays to identify homologous or heterologous recognition of linear epitopes.

Linear epitopes located within the RBD (peptides 15 to 18, 23 to 30) and wing domains (peptides 109 to 116) of MARV and RAVV GP were recognized by antibodies induced by either the MARV or RAVV vaccine (Fig. 6A, B). Moreover, the magnitude of vaccine-induced antibody binding to these epitopes in the homologous virus somewhat mirrored the magnitude of binding observed towards the same epitopes in the heterologous virus. The RBD is highly conserved between the marburgviruses. Peptides 15–18, 23–25 and 29–30 encompass part of the engagement site for the host receptor Niemann-Pick C1 and the footprint for neutralizing mAbs MR78 and MR191, isolated from human survivors[32] that provide post-exposure protection in animal models[29,31]. Peptides in the MARV GP2 wing domain recognized by both MARV- and RAVV-mRNA vaccine-specific antibodies encompass the epitopes for three mAbs: the two human mAbs, MR235 and MR228, and the murine mAb 30G4[27,33]. The peptide in the RAVV GP2 wing domain corresponding to the MR228 epitope was not recognized by MARV- and RAVV-mRNA vaccine-specific antibodies (peptide 112). MR228 failed to bind RAVV GP due to a two amino acid difference (aa 454T-455E) in the epitope compared to MARV GP (aa 454A-455P). This amino acid divergence appears to diminish the recognition potential of the humoral response towards RAVV.

Antibodies targeting linear epitopes in the MLD were unique to the respective virus, with MARV-MLD antibodies unable to recognize the RAVV-MLD and vice versa. RAVV vaccine-induced antibodies had a greater breadth of binding to the MLD than MARV-derived antibodies. The MLD is a poorly conserved region between the two viruses, and therefore, the lack of cross-recognition of MLD in heterologous viruses was not unexpected.

Interestingly, MARV mRNA vaccination induced antibodies with a greater capacity to bind the internal fusion loop (IFL) region of both MARV and RAVV, compared to the RAVV mRNA-vaccination. Weak recognition of the IFL by RAVV-vaccine antibodies indicates they have lower affinity than MARV-vaccine antibodies, the RAVV IFL is poorly ranked amongst the immunogenic B-cell epitope hierarchy, or the RAVV GP2 stem is somewhat obstructed[33]. MARV mRNA vaccination also induced antibodies with a greater capacity to bind the GP2 stem region of both MARV and RAVV GP compared to RAVV mRNA vaccination. Antibody recognition of the stem was generally weak, with only peptide 149 in the heptad repeat-1 (HR1) of both MARV and RAVV GPs showing the strongest binding in this region. While protective mAbs targeting the stem have not been identified for orthomarburgviruses thus far, an indication of rarity, mAbs specific for the GP stem of orthoebolaviruses have been isolated from human survivors[34].

The peptide arrays highlight regions within GP that are virus-specific and regions that are cross-reactive. While the antibody response following vaccination was greater in breadth and magnitude towards linear epitopes of the homologous virus, comparable magnitudes of binding were observed at cross-reactive epitopes. The strongest binding was observed for the RBD of GP1 and the wing domain of GP2. The linear epitopes recognized by cross-reactive, vaccine-induced antibody populations may be important contributors to their ability to cross-neutralize the two viruses.

The vaccines induce multiple Fc mediated effector functions

In addition to mechanical neutralization by antibodies, their Fc-mediated effector functions have been implicated in contributing to protection in vaccinated and natural infection survivors[35]. We examined the ability of the MARV- and RAVV-vaccine-induced immune sera to activate phagocytosis mediated by neutrophils (antibody-dependent neutrophil phagocytosis; ADNP) and monocytes (antibody-dependent cellular phagocytosis; ADCP). Antibody responses produced after MARV or RAVV mRNA vaccination activated virus-specific ADNP and ADCP functions in vitro. ADNP and ADCP activities were higher after prime MARV vaccination compared to after RAVV vaccination, but increased after the boost dose such that discernable differences were no longer observed between the two vaccines (Fig. 7A, B).

We also examined the ability of serum antibodies to facilitate antibody-dependent natural killer (ADNK) cellular cytotoxicity by measuring their markers for degranulation (CD107a) and activation (macrophage inflammatory protein-1β [MIP-1β] and interferon-γ [IFNγ]). Activation of the NK cellular activity was achieved by both vaccines (Fig. 7C–E). The MARV and RAVV boosters were required to activate similar levels of degranulation. The level of NK cells positive for MIP-1β comparably increased after prime vaccination with both vaccines and was further elevated by the booster dose. Almost no NK cells positive for IFNγ were detected after prime vaccination; unexpectedly, the levels increased after a booster of the RAVV mRNA but not the MARV mRNA. NK cells may control infection directly by their cytolytic functions and only partially by recruiting other immune cells through MIP-1β, rather than IFNγ production.

https://doi.org/10.1038/s41467-025-60057-0

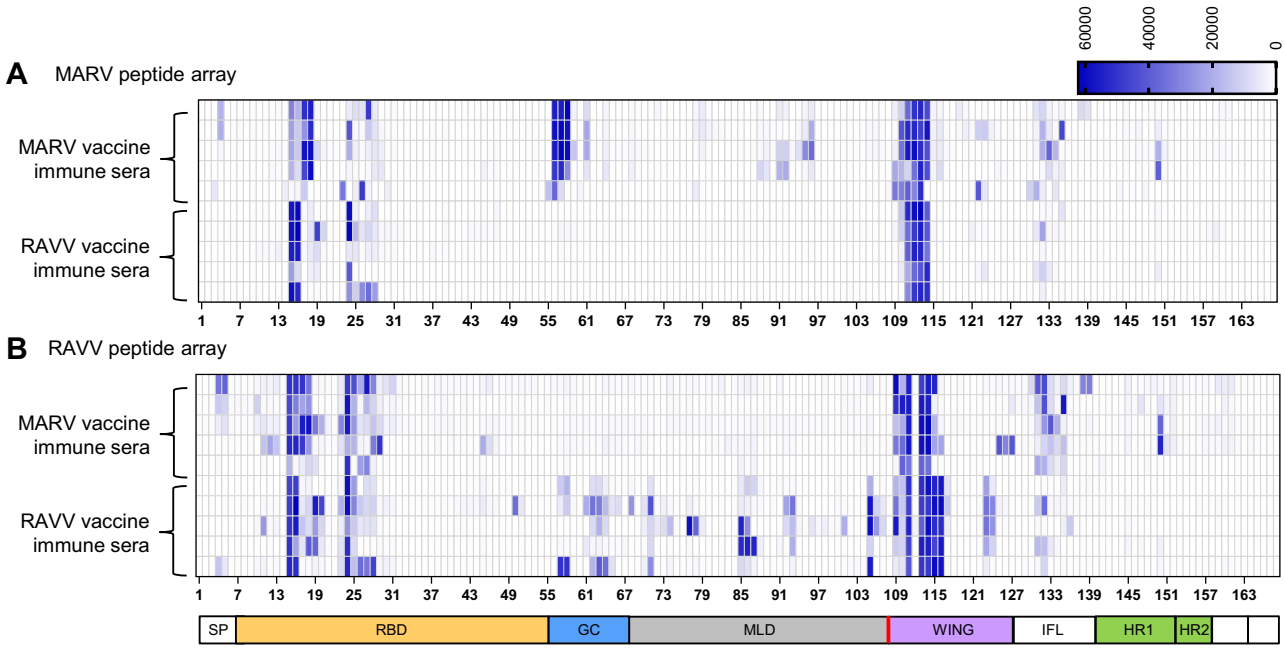

Fig. 6 | MARV and RAVV mRNA vaccines generate antibodies with different linear epitope profiles spanning full-length MARV or RAVV GP. The mean fluorescence intensity (MFI) of day 54 immune sera from each MARV or RAVV vaccinated guinea pig ($n = 5$ per vaccine group) binding individual peptides spanning (**A**) MARV or (**B**) RAVV GP plotted against each peptide (x-axis) in a heatmap. MFI baseline corrections were performed with immune sera collected from the same guinea pigs at day 0 prior to vaccination. The domain schematic of GP identifies the location of each peptide within GP. SP signal peptide (no color), RBD receptor binding domain (gold), GC glycan cap (blue), MLD mucin-like domain (gray), W wing (purple), IFL internal fusion loop (white), HR1 heptad repeat 1 (green), HR2 Heptad repeat 2 (green). Red line denotes the furin cleavage site. The vaccine constructs are indicated on the left y-axis of each heatmap. The heatmap scale represent the MFI value, whereby the intensity of blue indicates a higher value.

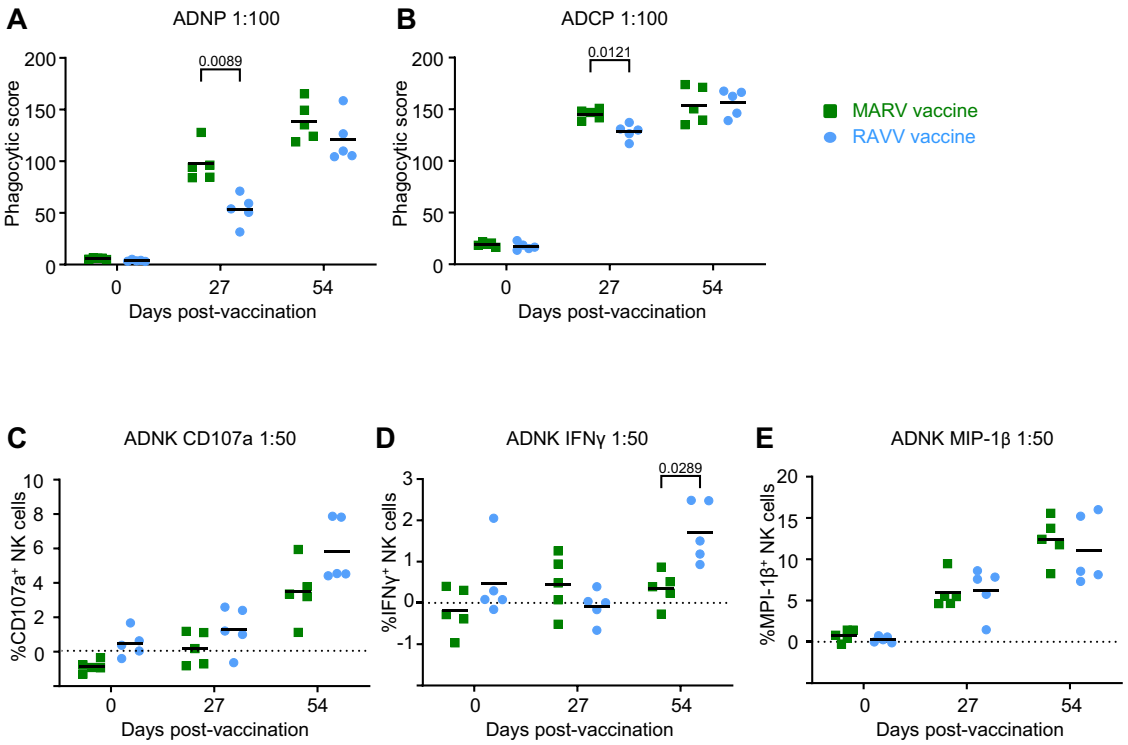

Fig. 7 | MARV and RAVV mRNA vaccines elicit Fc-mediated antibody responses. The level of (**A**) ADNP, (**B**) ADCP and (**C**–**E**) ADNK activity of immune sera at specified dilution, in guinea pigs grouped according to MARV (green square) or RAVV (blue circle) vaccine ($n = 5$ per vaccine) at days 0, 27 and 54 post-vaccination. NK cell activation data were measured according to production of (**C**) CD107a, (**D**) IFNγ and (**E**) MIP-1β and each data point is the average from two donor blood samples. **A**–**E** Significance was measured by repeated measures two-way ANOVA with Sidak's correction for multiple comparisons between vaccine groups.

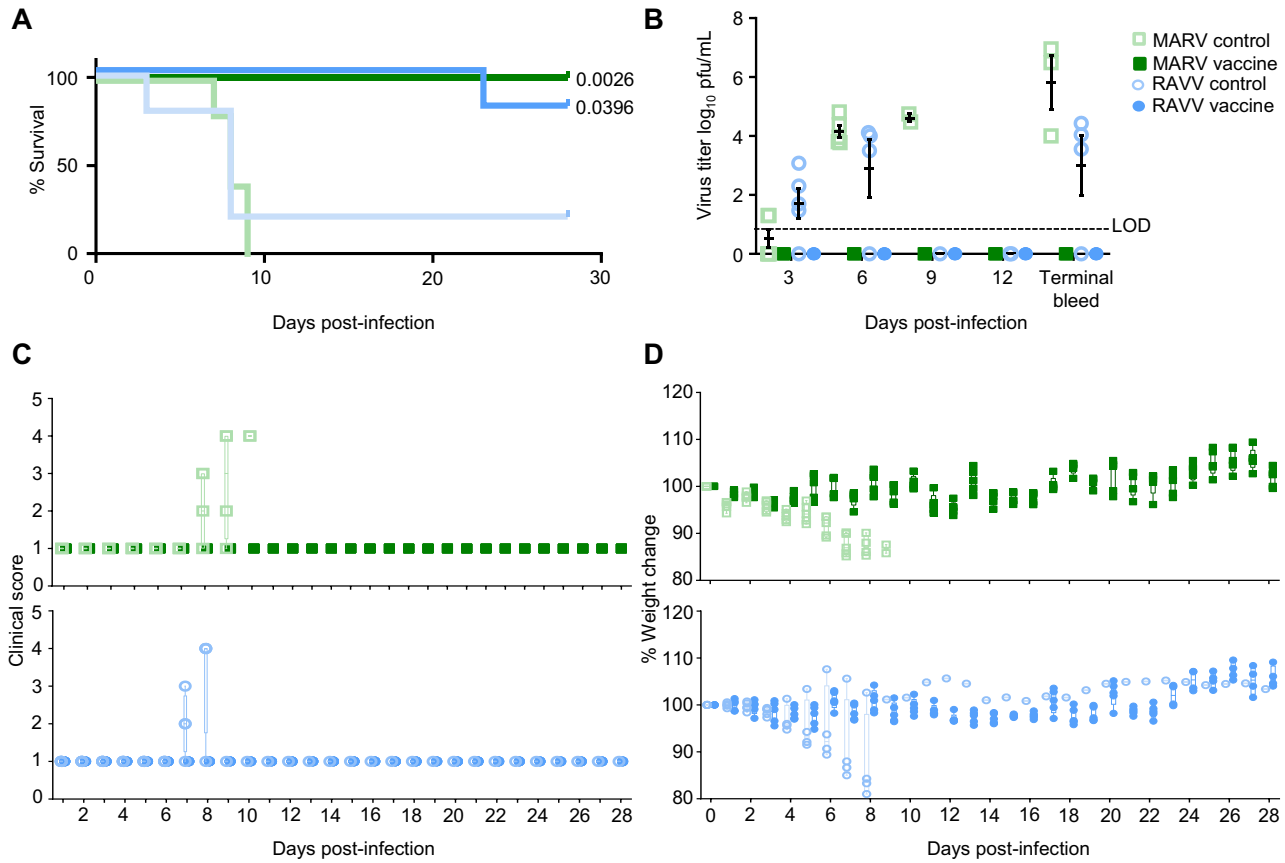

Fig. 8 | MARV and RAVV mRNA vaccines protect against homologous virus infection in guinea pigs. Guinea pigs ($n = 5$ per vaccine) recipients of the MARV mRNA (solid square), RAVV mRNA (solid circle) or mock ($n = 5$ per virus, square and circle outline) vaccines were challenged with 1,000 PFU of the corresponding guinea pig-adapted MARV (green) or RAVV (blue) by the intraperitoneal route. All animals were monitored for changes in (**A**) survival, (**B**) viremia, (**C**) clinical scores, and (**D**) % weight change over 28 days. **A** One RAVV vaccinated guinea pig was euthanized on day 23, due to a sustained physical injury. This animal maintained a steady weight and had no detectable virus during the infection phase and at the time of euthanasia. Two-sided Log-rank Mantel-Cox test for comparison of survival curves from mock and MARV or RAVV mRNA vaccine groups infected with the respective virus. **B** Serum was collected from all animals over the course of infection and measured for infectious virus by plaque titration (PFU/mL). Limit of detection (LOD). Bar denotes group mean values ± SEM. **C**, **D** The outer limits of the box reflect the interquartile range (IQR: Q3–Q1) with median shown as horizontal bars. Whiskers extend to minimum or maximum values.

mRNA vaccines protect against homologous MARV and RAVV infections

At day 56, guinea pigs were homologously challenged with 1,000 plaque-forming units (PFU) of guinea pig-adapted MARV variant Angola[36] or guinea pig-adapted RAVV[37] (Fig. 1). All guinea pigs vaccinated against MARV or RAVV survived infection (Fig. 8A). Over the 28-day infection phase, serum was collected at 3-day intervals for the first 12 days to measure viremia (Fig. 1). Guinea pigs were also monitored for clinical signs of disease including lethargy, neurological symptoms and weight loss. Vaccinated guinea pigs maintained steady weight over the infection phase, did not have detectable viremia, and displayed no signs of disease (Fig. 8B–D). One RAVV-vaccinated guinea pig sustained a physical injury unrelated to infection and was euthanized at day 23 (Fig. 8A). No virus was detected in the blood of this animal collected at the time of euthanasia (Fig. 8B). Control RAVV-infected guinea pigs developed severe disease and exhibited weight loss before succumbing to infection by day 9 (Fig. 8A, C, D). Four out of 5 MARV-infected control guinea pigs succumbed by day 8, and exhibited clinical disease and weight loss over the infection course. The shorter time to lethality with MARV infection compared to RAVV is consistent with its greater virulence observed in the guinea pig model[37]. The lack of detectable circulating virus in the surviving RAVV control guinea pig (Fig. 8B) may indicate imprecise administration of the infectious inoculum by intraperitoneal injection, a strict requirement to achieve uniform lethality.

mRNA vaccines protect against heterologous MARV and RAVV infections

The identification of cross-reactive antibody responses shared between the MARV and RAVV vaccines prompted us to explore the ability of the vaccines to cross-protect against heterologous challenge. Guinea pigs were vaccinated against MARV ($n = 10$), RAVV ($n = 10$) or mock vaccinated with PBS ($n = 10$) using a prime-boost regime that was shortened to 3-week intervals between the doses and the challenge (Fig. 9A). During the vaccination phase, GP-specific serum IgG were generated at levels that aligned with the first study (supplementary Fig. 3). At day 42, 5 of the 10 guinea pigs from each vaccinated group were challenged with guinea pig-adapted MARV and the other 5 were challenged with guinea pig-adapted RAVV (Fig. 9A). The homologous challenges served as quality controls for the vaccines, and the mock vaccinated guinea pigs served as controls for the challenge viruses. Serum was collected every 3 days for the first 12 days and at the day 28 study endpoint to measure viremia. Guinea pigs were monitored for clinical signs of disease according to the criteria outlined in the first study. Temperatures higher or equal to 40 °C were interpreted as a fever. All vaccinated guinea pigs challenged with the heterologous virus survived (Fig. 9B), showed no symptoms of disease (Fig. 9C) and maintained steady weights (Fig. 9D). All vaccinated guinea pigs that were homologously or heterologously challenged with MARV or RAVV maintained body temperatures below 40 °C with exception of one MARV- and one RAVV-vaccinated guinea pig, which experienced

https://doi.org/10.1038/s41467-025-60057-0

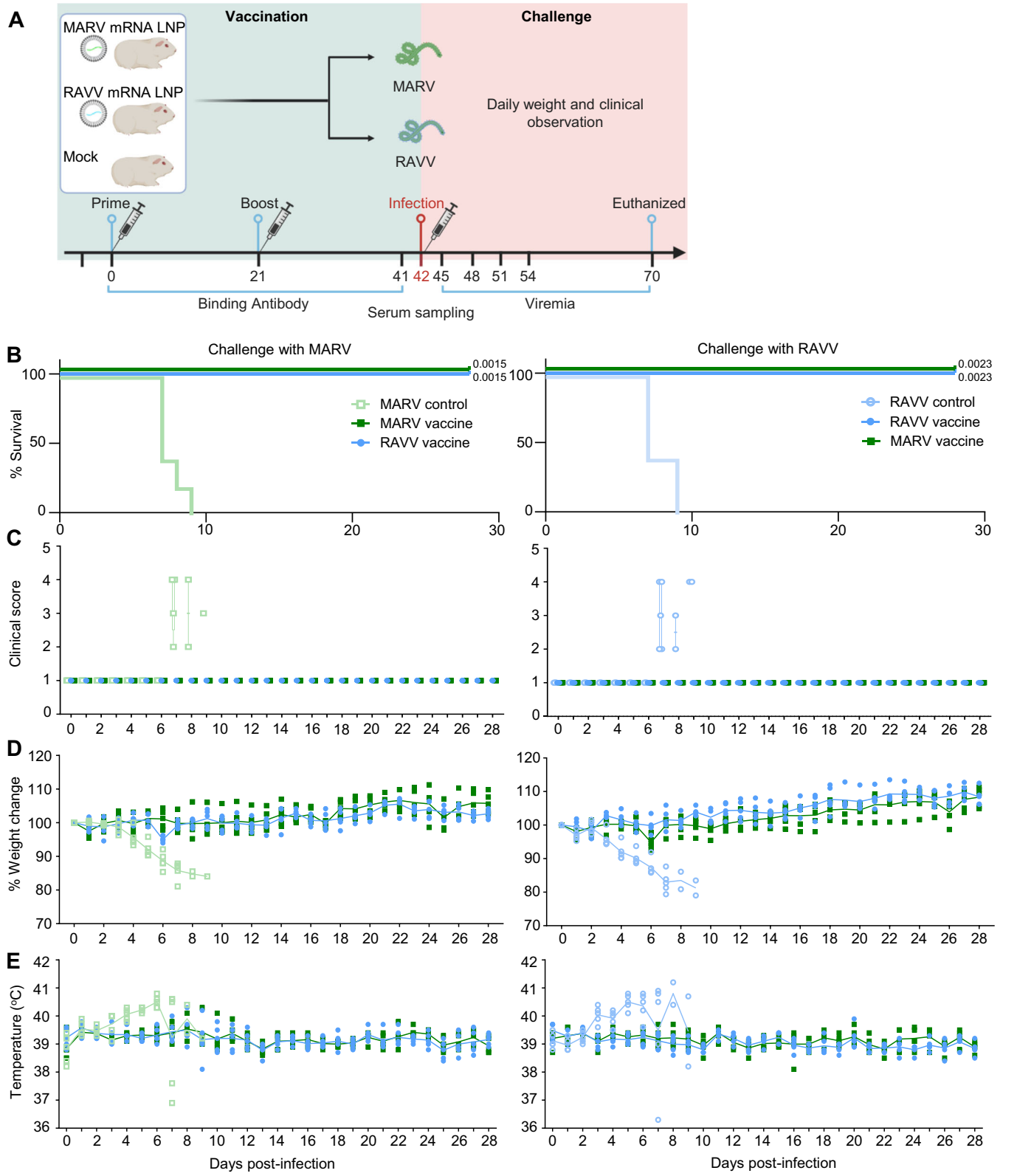

Fig. 9 | Both MARV and RAVV vaccines are cross-protective. A Schematic of cross protection study. Guinea pigs were vaccinated ($n = 10$ per vaccine group) via the intramuscular route on day 0 and boosted on day 21 with MARV mRNA (green) or RAVV mRNA (blue). Mock-vaccinated animals served as controls for infection. Guinea pigs from each vaccine group were challenged with 1000 PFU of guinea pig-adapted MARV or RAVV by the intraperitoneal route at day 42 ($n = 5$ per vaccine per virus). Created in BioRender. Meyer, M. (2025) https://BioRender.com/k70s169 **B**–**E** Recipients of MARV mRNA (green solid square), RAVV mRNA (blue solid circle) or mock controls for MARV (green square outline) and RAVV (blue circle outline) were infected with MARV or RAVV and monitored for changes in (**B**) survival, (**C**) clinical scores, (**D**) weight and (**E**) temperature over 28 days. **B** Two-sided Log-rank Mantel-Cox test for comparison of survival curves from mock and each vaccine group challenged with MARV or RAVV. **C** The outer limits of the box reflect the interquartile range (IQR: Q3–Q1) with median shown as horizontal bars. Whiskers extend to minimum and maximum values. **D**, **E** Line represents the mean value for each group.

temperatures slightly above 40 °C just outside the acute infection phase with MARV, before returning to baseline (Fig. 9E). The elevated temperatures did not coincide with weight loss but agrees with guinea pig-adapted MARV exhibiting greater virulence than guinea pig-adapted RAVV. Heterologously infected vaccinated guinea pigs did not have viremia detectable by plaque assay (supplementary Fig. 4). As expected, guinea pigs challenged with the homologous virus survived, while mock controls infected with MARV or RAVV succumbed to infection by day 9.

Shared antibody signatures are likely responsible for the cross-protective ability of both vaccines. Several features of the antibody response to MARV or RAVV vaccination in the guinea pigs homologously challenged in the first study differed at day 54 post vaccination, indicating a trade-off in protective mechanisms (Fig. 10A). MARV vaccination generated more antibodies binding to GPΔTM and the GC region than RAVV vaccination, while RAVV vaccination favored neutralizing antibodies, ADNK activity, antibodies binding to the combined RBD+wing+GP2 domains and GPcl, and responses to RBD epitopes for MR78, MR82 and MR198 antibodies. Features that were similar between MARV and RAVV vaccinations, including IgG titers, binding to MR72, MR191, and MR235 epitopes, and ADCP and ADNP activities, may contribute to cross-protection (supplementary Fig. 5). Pairwise correlation analysis of intra-vaccine associations of response features suggests the MARV and RAVV vaccines have distinct immune response patterns (Fig. 10B). A larger group sample number would increase confidence in identifying the associations involved in protection, and the intra-vaccine response patterns that may be involved in cross-protection. To identify relationships that could apply across both vaccines, features of their antibody responses were combined in a pairwise correlation analysis (Fig. 10C). Strong positive associations were observed between neutralizing titers and neutralizing antibody epitopes, or antibodies targeting the RBD, wing and GP2 regions. Positive associations were observed between neutralizing antibodies targeting the GPΔmuc domains and cross-neutralizing titers or ADNP, and between IgG titers and ADNP. These relationships were also somewhat evident for each vaccine suggesting they were general features of the immune response (Fig. 10B). In the combined correlation analysis, binding to the GC negatively correlated with features relevant to antibody neutralization, and cross-neutralizing titers negatively correlated with the MR82 epitope (Fig. 10C). However, since these associations only held true for the MARV vaccine and not the RAVV vaccine (Fig. 10B), the divergent response interplay was likely masked. This suggests that the relationship between the GC and neutralization and the contribution of the MR82 epitope towards cross neutralization may depend on the vaccine. While the GC may be a target for neutralizing antibodies generated by MARV vaccination (Fig. 4A), this relationship may be context-dependent, influenced by other immune factors since an abundance of GC antibodies did not equate to greater virus neutralization.

Discussion

The mRNA-LNP vaccines against MARV and RAVV we developed here successfully protected guinea pigs against death and severe disease caused by lethal challenge with the respective viruses. mRNA-LNP vaccines proved to be highly efficacious in preventing severe disease caused by infection with severe acute respiratory syndrome coronavirus-2 (SARS-CoV-2). However, mRNA-LNP vaccine-induced immunity against SARS-CoV-2 is non-sterilizing in humans and NHPs at its clinically-relevant dose[38] with limited durability that has enabled continued virus transmission and breakthrough infections by evolving variants of concern. An understandable level of uncertainty may surround the ability of mRNA-LNP vaccines to protect against a highly lethal pathogen, for which a robust, near-sterilizing immune response is crucial for preventing disease progression. While filoviruses do not mutate as fast as coronaviruses in the field during outbreaks, curbing virus replication becomes increasingly important as filoviruses are highly transmissible. In our study, the immunity conferred by mRNA-LNPs vaccination was potentially sterilizing, as both orthomarburgviruses remained undetectable in circulation. The mRNA-encoded marburgvirus GP antigen appears to be sufficiently immunogenic to achieve sterilizing immunity.

We sought to characterize the antibody responses to both vaccines to determine similarities and differences in their profiles, given the sequence divergence between MARV and RAVV GPs. While mRNA vaccine sequences are easily tailored to target the pathogen of concern, a vaccine that can generate a cross-protective immune response is highly desirable. The frequency of the antibody response towards certain GP domains differed between the two vaccines. The MARV mRNA vaccine generated a greater frequency of antibodies that targeted the GC than the RAVV mRNA vaccine. Moreover, recognition of homologous peptides in the GC was more evident with the MARV vaccine response, indicating that this region may be more immunogenic in MARV variants than in RAVV. The proportion of the total antibody response towards the MLD was similar between the RAVV and MARV vaccines. However, the breadth of recognition towards autologous linear MLD epitopes was greater for RAVV vaccine recipients, suggesting the sequence heterogeneity within the MLD shaped the epitope-recognition profile without affecting the binding frequency.

Differences between MARV and RAVV vaccine-derived neutralizing antibody responses were also identified. RAVV mRNA vaccination appeared to generate more neutralizing antibodies towards the furin cleaved form of GP (GPcl), rather than the un-cleaved structure of GP lacking the MLD (GPΔmuc), a finding that may be attributed to the RBD epitopes exposed following the removal of the GC structure. On the other hand, the MARV mRNA vaccine appeared to generate a greater neutralizing response towards GPΔmuc than GPcl. Therefore, GC epitopes appear to be involved in the neutralizing activity against MARV; GC antibodies in serum that were not removed by pre-adsorption with GPcl (which lacks the GC) could neutralize the virus. The strength of linear epitopes recognition in the GC of MARV, but not RAVV, vaccine recipients, indicates that it is a virus-specific immunogenic region. It was previously suggested that mAbs recognizing the regions in proteolytically cleaved GP, in addition to the RBD, were involved in virus neutralization[27]. Neutralizing mAbs from MARV survivors are rare and diminish over time[39,40]. While no GC-specific mAbs from survivors have been described in the literature thus far, the possibility of their existence cannot be ruled out given our findings of linear epitope footprints and the large portion of vaccine-derived antibodies directed to the region. The GC of MARV GP appears to shape the serum antibody response profile more so than the GC of RAVV GP, eliciting higher antibody frequencies, neutralizing capacity and linear epitope recognition. Conversely, the combined RBD, wing and GP2 domains of RAVV GP generated proportionally greater antibody binding and neutralizing responses compared to MARV. Unlike orthoebolaviruses, the GC structure of orthomarburgviruses appears disordered, such that the RBD domain is exposed even prior to cathepsin cleavage[29]. The GP of MARV and RAVV are thought to have similar structures. However, the RAVV GP structure is more stable compared to MARV GP[33]. Our results suggest that sequence evolution may influence a structural divergence between GPs of distant orthomarburgviruses by potentially affecting stability, modifications[41], and/or the spatial location of domains. The crystal structures of GP from closely related orthoebolaviruses, EBOV and SUDV, highlighted electrostatic differences which may be responsible for their opposing susceptibility to endosomal proteases[42]. In this study, the intact MARV GP appeared more immunogenic than its proteolytically-cleaved structure, promoting a GC-heavy response. The proteolytically cleaved form of RAVV GP appeared more immunogenic than its full structure. Structural divergence may also explain the varied responses towards the RBD, IFL

https://doi.org/10.1038/s41467-025-60057-0

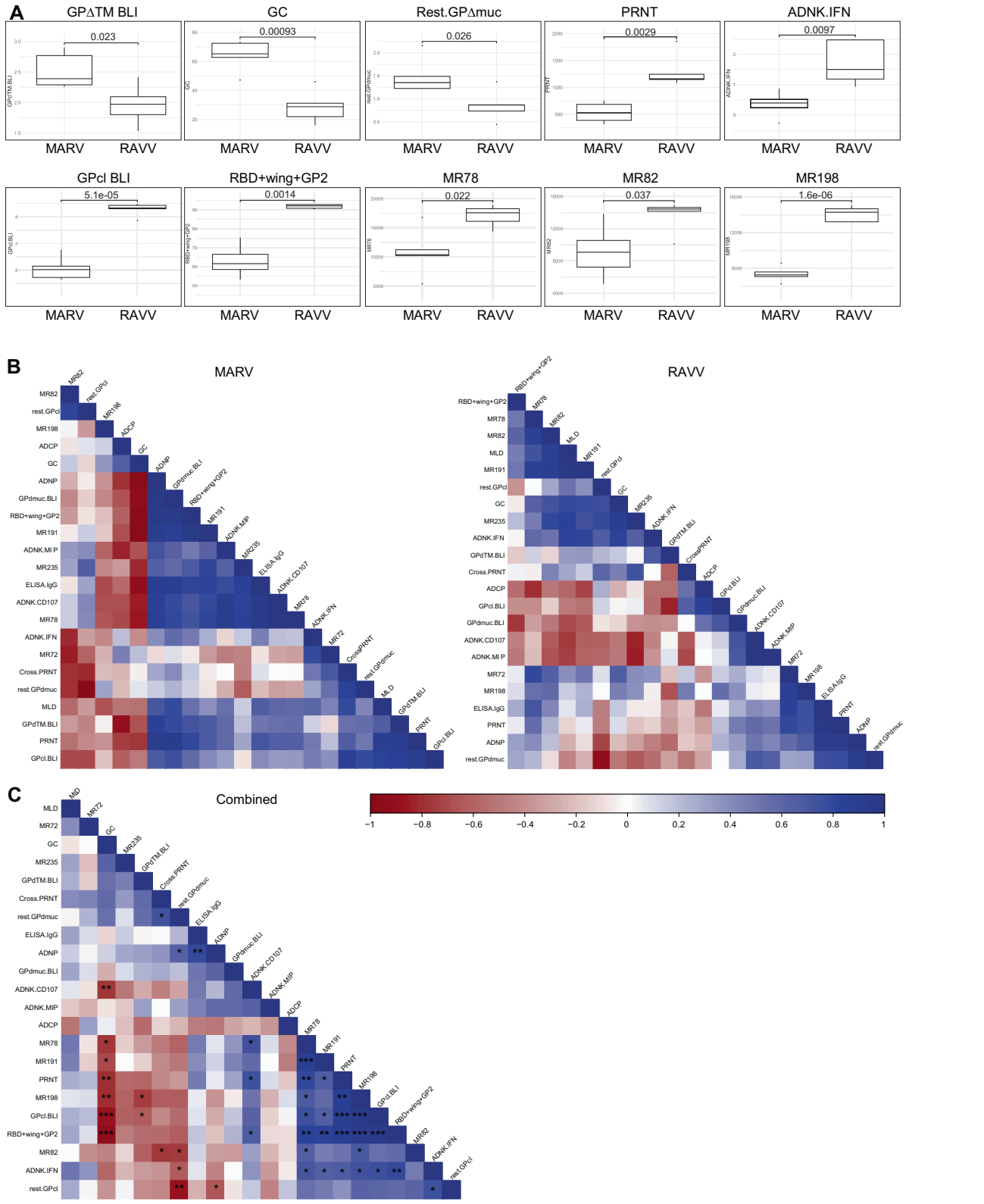

Fig. 10 | Correlation analysis identifies divergent immune relationships between MARV and RAVV vaccines. A Unpaired, two-sided Welch's *t*-test results for differential immune response parameters generated in the homologous challenge guinea pig cohort at day 54 post vaccination with MARV and RAVV mRNA ($n = 5$ per vaccine group). The outer limits of the box reflect the interquartile range (IQR: Q3–Q1) with median shown as horizontal bars. Whiskers extend to 1.5 times the IQR of the box. Outliers outside 1.5 × IQR are shown as individual points. **B**, **C** Heatmap two-tailed Pearson's correlation matrix depicting pairwise associations between parameters measured at day 54 post vaccination for (**B**) each MARV or RAVV vaccine ($n = 5$ per vaccine group) or for (**C**) combined MARV and RAVV vaccines ($n = 10$). Pearson's correlation coefficient values, where color intensity indicate higher correlation, and color represents direction of correlation: positive, blue; negative, red. $P \le 0.05$, $^{**}P \le 0.01$ and $^{***}P \le 0.001$. Exact (**B**, **C**) correlation coefficient and (**C**) *p*-values are reported in the Source Data file.

or the GP2 stalk regions of MARV and RAVV despite these sites sharing nearly 100% sequence homology.

Previously, protective mAbs from survivors targeting the wing domain were shown to possess Fc-effector functions. In another study, the wing domain elicited protective antibodies in mice with partial in vitro neutralizing activity[33]. We show that the wing domain may be a major target for recognition by neutralizing serum antibodies. Removal of RBD, GC, and GP2 antibodies in sera from RAVV vaccinated animals by pre-absorption with GPΔmucΔw did not eliminate virus neutralization. Therefore, antibodies can directly target the wing domain for neutralization, and not just affect a conformational change in GP that enables access by RBD-neutralizing antibodies[27]. The MLD domain of GP encoded by both the MARV and RAVV mRNA vaccines appeared to contribute minimally to the neutralizing potential of the humoral response.

The linear epitope footprint encompassing MR228 and MR235 in the GP2 wing region was a prominent site recognized by MARV and RAVV vaccine-induced serum antibodies. Despite MR228 and MR235 having overlapping epitopes, the MARV mRNA vaccine-directed response towards the MR228 epitope exceeded that of MR235. The frequency of antibodies in MARV-vaccinated recipients targeting the MR228 epitope was greater than that targeting RBD epitopes, while the frequency of antibodies targeting the MR235 epitope was similar to RBD antibodies. This conflicts with previous findings in which the prevalence of wing domain antibodies in the serum of human MARV survivors was lower compared to RBD antibodies[27]. However, for RAVV mRNA vaccine recipients, the frequency of most RBD-specific antibodies was generally higher than MR235. MR228 is a non-neutralizing mAb that uses Fc-effector functions to protect animals from lethal infection, potentially highlighting the importance of its epitope in directing cell-mediated immune responses[43]. The varying responses to RBD and wing domain mAb epitopes generated by the two vaccines points to an epitope-driven disparity influencing the functional antibody profile.

Antibody-dependent cellular functions contribute to protection against MARV infection in the absence of detectable neutralizing activity[44]. Both MARV- and RAVV-vaccine-derived serum antibodies facilitated ADCC activity to a similar extent after booster doses. However, antibodies with phagocytic potential were induced faster in MARV recipients compared to RAVV recipients, despite both vaccines eliciting similar IgG kinetics (Fig. 3). Superior antibody-mediated cellular phagocytosis observed in MARV-recipients and neutralizing activity in RAVV-recipients, suggest that differences in the GP regions targeted by the two vaccines may influence antibody functionality and protective mechanisms. The apparent greater phagocytic potential of MARV vaccine-derived antibodies may be attributed to a somewhat skewed recognition intensity toward linear epitopes and protective mAb epitopes in the wing domain compared to those in the RBD. The wing domain, part of GP2 equatorially projected on GP, is thought to be recognized primarily by antibodies with Fc-mediated effector functions, given its spatial accessibility to immune cells[27]. The epitopes of human survivor mAbs with ADCC functions were targeted by serum antibodies from our mRNA-vaccinated guinea pigs. Fc effector functions likely contribute to the protection conferred by the vaccines, but the extent of their contribution and the exact protective mechanisms may differ between the two vaccines.

Increasing evidence suggests T cell responses are involved in protection against filoviruses[11,39]. mRNA vaccines are known to activate T cells[45–47], and the epitopes of T cells induced by mRNA vaccines capable of homologous and heterologous protection need to be interrogated. However, humoral responses to filovirus vaccination correlate with protection, and antibody treatment studies have been successful in NHPs, signifying their importance. To date, the known protective mAbs against orthomarburgviruses sourced from human survivors or vaccinated animals were mapped to the RBD and GP2 regions of MARV, with human-derived neutralizing mAbs targeting only the RBD, a fraction of the regions reported for EBOV. This suggests the MARV GP structure, response durability, or antibody isolation or vaccination strategies may constrain antibody discovery. With immune similarities to humans and recapitulation of filovirus pathogenesis, guinea pigs are an archetypical model to evaluate vaccine candidates and support further studies in NHPs[48]. Antibodies raised in guinea pigs can recognize antigens similarly to human antibodies, with potentially diverse specificities that exceed other rodent models[49,50]. Rare antibodies that would otherwise be diluted in polyclonal responses are being discovered in guinea pigs through antigen deconvolution to broaden antibody treatment options and facilitate vaccine design[51,52]. Therefore, it may be possible to expand the MARV antibody repertoire through further exploration in animal models such as guinea pigs.

The ability to induce cross-protection against both orthomarburgviruses appears to depend on the vaccine platform. A Venezuelan equine encephalitis virus replicon vaccine against MARV (variant Musoke) failed to protect against RAVV[53,54]. Conversely, a VSV-vectored MARV vaccine (variant Musoke) did confer protection against RAVV[55]. We showed that while the RAVV mRNA vaccine promoted somewhat better cross-neutralization than the MARV mRNA vaccine, both vaccines were able to protect against heterologous virus challenge. Peptide array analysis identified common linear peptides within two regions of GP, the RBD and wing, that were recognized by cross-reactive antibodies induced by MARV or RAVV vaccination. This suggests that these immunogenic epitopes shared between the two viruses may be responsible for cross-protection, although cross-protective epitopes may rely on GP conformation[25,29]. Antibody response patterns that were robust across both vaccines may also indicate core immune mechanisms involved in cross protection. Therefore, mRNA vaccines have the potential to induce broadly cross-reactive responses. Future challenge studies with vaccine constructs modified at the epitopes of interest will be necessary to identify the epitopes responsible for cross-protection.

The differences in antibody reactivity and functionality profiles between the two orthomarburgvirus vaccines we identified in this study are equally important as they are insights into potential structural differences in the targeted GP antigens. These differences potentially influence responses towards regions with sequence homology between viruses, which under normal conventions, would elicit similar immune responses. These findings may have fundamental implications in designing cross-protective vaccines. Our promising results against EBOV previously[19], and now against MARV and RAVV, support future preclinical efficacy testing of the mRNA-LNP platform in the stringent NHP model.

Methods

mRNA synthesis and nanoparticle formulation

mRNA vaccines were synthesized in vitro by T7 polymerase-mediated transcription with substituted 1-methylpseudo UTPs, using linearized DNA templated encoding GPs from MARV isolate Angola05, GenBank accession number: DQ447653.1 and RAVV (isolate Kenya 1987, GenBank accession number: DQ447649.1). The wild-type signal sequence of GP and 5′ and 3′ untranslated regions (UTRs)[30] were incorporated into the mRNAs. The mRNAs were purified and resuspended in a citrate buffer at the desired concentration. A donor methyl group S-adenosylmethionine (SAM), was added to methylated capped RNA (cap-0), resulting in a cap-1 structure to increase mRNA translation efficiency[56]. LNP formulations were prepared as previously described[30].

Testing of the immunogenicity and protective efficacy in guinea pigs

For the homologous virus challenge study, 8-week-old female guinea pigs, strain Hartley ($n = 5$ per group), were intramuscularly vaccinated in the left hind leg on days 0 and 27 with 0.1 mL of MARV or RAVV mRNA vaccines (40 µg). Two groups were mock-vaccinated with PBS to serve as the MARV or RAVV infection controls. On day 56, the mock-vaccinated and vaccinated groups were intraperitoneally infected with 1000 PFU of the respective guinea pig-adapted MARV, provided by Dr. G. Kobinger while at the National Microbiology Laboratory, Winnipeg, Canada[36] or RAVV[37]. Guinea pig-adapted MARV was originally isolated from a patient in Angola, passaged once in Vero-E6 cells, eight times in Hartley guinea pigs using liver and spleen homogenates, once in Vero PP cells, and once in Vero cells for stock production. Guinea pig-adapted RAVV was developed by 2 passages in strain 13 guinea pigs and 1 passage in Hartley guinea pigs. Serum was collected days 0, 27, and 54 post-vaccination and at 3-day intervals over 12 post-infection days, and at day 28 post-infection, the time of euthanasia.

For the heterologous virus challenge study, 8-week old female Hartley guinea pigs were vaccinated against MARV, RAVV or mock vaccinated with PBS ($n = 10$ per group) as described above with the exception of using a prime-boost schedule spaced 3 weeks apart (Fig. 9A). Serum was collected prior to each vaccination and challenge to verify the IgG response. At day 42, 5 of the 10 guinea pigs from each group were challenged with MARV and the other 5 were challenged with RAVV (Fig. 9A). The post-challenge serum collection and euthanasia schedule was consistent with the homologous virus challenge study. Upon infection, the guinea pigs were monitored at a minimum once-daily for temperature (heterologous study only) and weight changes and scored clinically, whereby a score 1 represented a healthy animal and score 4 required euthanasia. All animal experiments were approved by the University of Texas Medical Branch Institutional Animal Care and Use Committee. Guinea pigs were housed in ABSL-2 during the vaccination phase of the study and transferred to ABSL4 prior to virus challenge.

Analysis of viremia

Vero-E6 cells were inoculated with serum, 10-fold serially diluted in MEM (Thermo Fisher Scientific) containing 0.05 mg/mL gentamicin (Thermo Fisher Scientific). After 1 h absorption at 37 °C, the inoculum was replaced with carboxymethyl cellulose overlay. Plates were incubated for 4 days before monolayers were fixed with formalin, and plaques were immunostained. Briefly, plates were blocked with PBS containing 5% nonfat dry milk for 1 h at 37 °C, followed by the addition of human mAbs, MR235 and MR186 (provided by Dr. James E. Crowe) diluted to 0.5 µg/mL in blocking buffer. Bound antibody was detected using secondary goat anti-human HRP conjugate (1:2,000 dilution, SeraCare) and ImmPACT AEC colorimetric substrate (Vector Laboratories).

Plaque reduction assays

Plaque reduction neutralization assays were performed as previously described[19]. Viruses used for neutralization-based assays were derived from MARV strain 200501379 Angola, isolated during the 2005 outbreak in Angola, and RAVV, isolated in Kenya in 1987[57,58]. Both viruses were passaged three and four times, respectively, in Vero E6 cells. Briefly, 2-fold serial dilutions of heat-inactivated serum, starting at 1:10, were prepared in MEM supplemented with guinea pig complement and incubated with virus for 1 h at 37 °C at a final concentration of 100 PFU and 5% complement. Dilutions of MR186 and MR198 human mAbs, known to possess neutralizing activity for MARV and RAVV, respectively, starting at 200 µg/µL, were included as positive controls in the assay. Virus-serum mixtures then were absorbed onto Vero-E6 monolayers for 1 h at 37 °C and replaced with MEM overlay. After 4 days, plates were fixed and immunostained as described above. Plaques were counted, and the serum antibody dilutions which achieved 60% neutralization were calculated.

Enzyme linked immunosorbent assays

ELISAs were performed as described[19] with modifications. Briefly, 96-well high binding microlon plates (Greiner) were coated overnight at room temperature with 8 ng per well of MARV (variant Angola; IBT Bioservices) or RAVV GPΔTM (provided by Dr. Erica Ollmann Saphire). Plates were blocked with 3% milk powder in PBS. Sera, diluted 4-fold in blocking solution starting at 1:16, were added to the plate. A peroxidase-labeled goat anti-guinea pig IgG (1:5000 dilution; Jackson ImmunoResearch Laboratories) detected bound antibodies. Blocking and binding steps with sera or secondary antibodies were performed at 37 °C for 1 h.

Serum binding and competition assays

A FortéBio Octet Red96 instrument (Sartorius) was used to measure serum antibody binding to MARV or RAVV GPs and their intermediate forms: MARV and RAVV GPΔTM, GPΔmuc and GPcl (provided by Dr. Erica Ollmann Saphire) and RAVV GPΔmucΔw (provided by Dr. James E. Crowe, Jr)[33]. All assays were performed with agitation at 1000 rpm, at 28 °C in black 96-well plates. All samples were diluted in 1× Kinetics buffer (FortéBio) with a final volume of 200 µL per well. Biotinylated GPΔTM, GPΔmuc (Δ257-425), GPΔmucΔw (additional residues Δ436-483) or GPcl were immobilized onto streptavidin sensors for 300 s to capture ~1 nm, with variability within a row of sensors not exceeding 0.1 nm. Biosensor tips were then equilibrated for 300 s in 1× Kinetics buffer before binding measurements. Sera were diluted 1:50, and binding was assessed for 600 s, followed by dissociation for 600 s in 1× Kinetics buffer. Parallel corrections for baseline drift were made by subtracting measurements recorded with GP-loaded sensors in the absence of sera. Non-specific sera binding was accounted for by running sera from mock-vaccinated controls alongside sera from vaccinated guinea pigs.

For pre-adsorption studies, sensors were treated with biocytin for 120 s after immobilization of a biotinylated GP form. Sera depleted with excess amounts of GP forms of MARV (5 µg GPΔTM and GPΔmuc, and 2.5 µg GPcl) or GP forms of RAVV (7.5 µg GPΔTM and GPΔmuc, 5 µg GPΔmucΔw and 1 µg GPcl) were allowed to bind to sensors as described above. To determine nonspecific binding responses, binding of sera from mock-vaccinated animals to GP variant-loaded probes was monitored and set as the background. We calculated the percent inhibition of binding to an immobilized GP after serum adsorption relative to the binding observed without pre-adsorption using the following formula: % inhibition = 100 − ([binding of serum pre-adsorbed with GP form (nm)/binding of serum without pre-adsorption (nm)] × 100). The percent inhibition values, derived from one immobilized GP variant as the common denominator, were used to calculate the relative proportions of serum binding to a specific GP domain.

For site-specific antigenicity assessment, GP-loaded sensors (captured at ~0.5 nm) were incubated with serially diluted serum in 1× Kinetics buffer for 900 s to generate a saturating signal against the competing mAb. Probes were then washed for 120 s before the reactivity of competing mAbs specific for the RBD (MR72, MR78, MR82, MR111, MR191 and MR198) or wing domain (MR228 and MR235) was assessed for 600 s. All mAbs recognize both MARV and RAVV, except for MR111 and MR228 which were specific for RAVV or MARV, respectively. GPΔmuc-loaded sensors were used for competition with all mAbs except MR235 which only bound GPΔTM. For MARV samples, 500 nM of MR72, MR78, MR82 and, MR191; 200 nM MR198 and MR228; and 10 nM MR235 were used for competition. For RAVV samples, 200 nM of MR72, MR78, MR82, MR111, MR191 and MR235; and 100 nM MR198, were used. Data analysis and curve fitting were carried out using Octet software, version 7.0. At each serum dilution, the binding inhibition to GP was calculated as a percentage of blocking by

sera from vaccinated animals relative to mock-vaccinated control sera against the tested mAb. The area under the curve (AUC) was calculated for binding inhibition values across the dilution series, following normalization to the initial lowest dilution.

Reversing neutralizing activity in the presence of GP forms

Competition neutralization assays were performed as previously described[59]. Briefly, day 54 sera diluted to concentrations that neutralized at least 70% of MARV or RAVV were incubated in duplicate with increasing concentrations of MARV or RAVV GPΔmuc or GPcl. GPΔmucΔw was also included for RAVV-specific serum. Preabsorbed serum was then exposed to virus in a neutralization assay. The ability of GP forms to reverse the neutralizing activity of serum (restoration of virus infectivity) was calculated as a percentage of the plaques formed in the presence of serum incubated with the competing GP forms compared to serum without the GP forms.

Binding of the immune sera to peptide microarrays

Peptide microarrays were used to map the linear epitopes in MARV and RAVV GPs recognized by the humoral response to vaccination. A microarray slide consisted of 21 blocks to enable analysis of up to 20 samples and one secondary antibody control. Each block was spotted with 168, 15-meric peptides offset by 4 amino acids, spanning the 681 amino acids of GP of MARV variant Angola (UniProtKB/Swiss-Prot: Q1PD50.1) or RAVV (NCBI Reference sequence: YP_009055225.1), as triplicate subarrays, by JPT Peptide Technologies GmbH (J.P.T.). Serum diluted 1:200 in wash buffer (J.P.T.) was applied to individual chambers on the slides and incubated for 1 h at 30 °C. Following 4 washes, slides were incubated with 0.1 µg/mL anti-guinea pig IgG Cy5-conjugated antibodies (Jackson ImmunoResearch Laboratories). After additional washes and a final rinse in deionized water, the slide was dried by centrifugation. Slides were scanned with the GenePix 4200AL using the 635 nm laser at 500 PMT and 100 Power settings. The fluorescent intensities for each spot of the array image were analyzed by GenePix Pro 7 (Molecular Devices), and the MFI across the triplicate sub-arrays for each block was calculated and normalized by subtraction from the secondary antibody control. Sera from all animals per group were tested, and normalized MFIs for each peptide were corrected for baseline by subtracting the corresponding pre-vaccination MFIs.

Fc-medicated effector functions

Antibody-dependent NK cell degranulation: Recombinant MARV or RAVV GP (IBT Bioservices) was coated onto MaxiSorp 96-well plates (Nunc) at 300 ng/well at 4 °C for 18 h. The wells were washed three times with PBS and blocked with 5% bovine serum albumin in PBS. Sera from immunized guinea pigs diluted 1:50 in PBS were added, and the plates were incubated for 2 h at 37 °C. Unbound antibodies were removed by washing three times with PBS, and NK cells freshly isolated from peripheral blood from two healthy human donors (collected at the Ragon Institute or the Massachusetts General Hospital Blood bank with signed informed consent and approval by the Massachusetts General Hospital Institutional Review Board) by negative selection (Stem Cell Technologies) were added at 5×10^4 cells/well in the presence of 4 µg/mL brefeldin A (Sigma-Aldrich), 5 µg/mL GolgiStop protein transport inhibitor (Life Technologies, Carlsbad, CA), and anti-CD107a antibody (1:40 phycoerythrin [PE]-Cy5; clone H4A3; BD Biosciences). The plates were incubated for 5 h. Cells were stained with anti-CD3 (1:100 Alexa Fluor 700; clone UCHT1; BD Biosciences), anti-CD16 (1:100 allophycocyanin [APC]-Cy7; clone 3G8; BD Biosciences), and anti-CD56 (1:100 PE-Cy7; clone B159; BD Biosciences), followed by fixation and permeabilization with the Fix & Perm reagent (Life Technologies) according to the manufacturer's instructions to stain for intracellular IFN-γ (1:50 APC; clone B27; BD Biosciences) and MIP-1β (1:50 PE; clone D21-1351; BD Biosciences).

Antibody-mediated neutrophil (ADNP) or cellular (monocyte, ADCP) phagocytosis: Recombinant MARV GP or RAVV GP were biotinylated using Sulfo-NHS-LC-LC biotin (Thermo Fisher Scientific) and coupled to 1-µm FITC+ NeutrAvidin beads (Life Technologies). Sera from vaccinated guinea pigs were diluted 1:100 in cell culture medium and incubated with GP-coated beads for 2 h at 37 °C. Neutrophils isolated from donor peripheral blood were added at a concentration of 5.0×10^4 cells/well, and the plates were incubated for 1 h at 37 °C. The cells were stained at 1:100 with CD66b (Pacific Blue; clone G10F5; BioLegend), CD3 (Alexa Fluor 700; clone UCHT1; BD Biosciences), and CD14 (APC-Cy7; clone MφP9; BD Biosciences). Neutrophils were defined as positive for a high side scatter area (SSC-Ahigh), CD66b + , CD3 − , and CD14 − . ADCP was measured as previously described[60] using a human monocyte cell line (THP-1 cells). Briefly, THP-1 cells (2.0×10^4 cells per well) were incubated for 18 h at 37 °C with the GP-coated FITC bead-serum mixtures in duplicate. All cells were fixed with 4% paraformaldehyde.

Stained cells from ADNK, ADNP and ADCP assays were analyzed by flow cytometry on a BD LSRII flow cytometer (supplementary Fig. 6), and a minimum of 30,000 (ADNP) or 10,000 (ADCP) events were recorded and analyzed. The phagocytic score was determined using the following formula: [(percentage of FITC+ cells) × (median fluorescent intensity [MFI] of the FITC+ cells)]/10,000.

Statistics

Statistical tests to determine the *p*-values were calculated using GraphPad software, Inc. and are indicated in the figure legends. R version 2023.09.0 Build 463 (Posit Software, PBC) was used for the analyses and visualization of Pearson's pairwise correlation heatmaps and Welch's *t*-tests. Normalization was checked through the generation of Q-Q plots prior to any analysis to determine correct statistical test selection. After confirming normalization with $n = 5$ per group, Welch's *t*-tests were performed using base R to compare groups. The Hmisc package was employed to compute correlation matrices using Pearson's correlation. All statistical significance was evaluated at $p < 0.05$ for every test.

Reporting summary

Further information on research design is available in the Nature Portfolio Reporting Summary linked to this article.

Data availability

Datasets generated and/or analyzed during the current study are provided with the paper or are appended as supplementary data. Source data are provided with this paper.

References

1. WHO. 2023. Equatorial Guinea confirms first-ever Marburg virus disease outbreak. https://www.afro.who.int/countries/equatorial-guinea/news/equatorial-guinea-confirms-first-ever-marburg-virus-disease-outbreak.
2. WHO. 2023. Tanzania confirms first-ever outbreak of Marburg Virus Disease. https://www.afro.who.int/countries/united-republic-of-tanzania/news/tanzania-confirms-first-ever-outbreak-marburg-virus-disease.
3. WHO. 2021. Marburg virus disease. https://www.who.int/news-room/fact-sheets/detail/marburg-virus-disease.
4. Swenson, D. L. et al. Monovalent virus-like particle vaccine protects guinea pigs and nonhuman primates against infection with multiple Marburg viruses. *Expert Rev. Vaccines* **7**, 417–429 (2008).
5. Callendret, B. et al. A prophylactic multivalent vaccine against different filovirus species is immunogenic and provides protection from lethal infections with Ebolavirus and Marburgvirus species in non-human primates. *PLoS One* **13**, e0192312 (2018).

6. Dye, J. M. et al. Virus-like particle vaccination protects nonhuman primates from lethal aerosol exposure with Marburgvirus (VLP vaccination protects macaques against aerosol challenges). *Viruses* **8**, 94 (2016).
7. Hunegnaw, R. et al. A single-shot ChAd3-MARV vaccine confers rapid and durable protection against Marburg virus in nonhuman primates. *Sci. Transl. Med.* **14**, eabq6364 (2022).
8. Swenson, D. L. et al. Vaccine to confer to nonhuman primates complete protection against multistrain Ebola and Marburg virus infections. *Clin. Vaccin. Immunol.* **15**, 460–467 (2008).
9. Woolsey, C. et al. A highly attenuated Vesiculovax vaccine rapidly protects nonhuman primates against lethal Marburg virus challenge. *PLoS Negl. Trop. Dis.* **16**, e0010433 (2022).
10. Jones, S. M. et al. Live attenuated recombinant vaccine protects nonhuman primates against Ebola and Marburg viruses. *Nat. Med.* **11**, 786–790 (2005).
11. Marzi, A. et al. Protection against Marburg virus using a recombinant VSV-vaccine depends on T and B cell activation. *Front Immunol.* **9**, 3071 (2018).
12. Clarke, D. K. et al. Safety and immunogenicity of a highly attenuated rVSVN4CT1-EBOVGP1 Ebola virus vaccine: a randomised, double-blind, placebo-controlled, phase 1 clinical trial. *Lancet Infect. Dis.* **20**, 455–466 (2020).
13. Hamer, M. J. et al. Safety, tolerability, and immunogenicity of the chimpanzee adenovirus type 3-vectored Marburg virus (cAd3-Marburg) vaccine in healthy adults in the USA: a first-in-human, phase 1, open-label, dose-escalation trial. *Lancet* **401**, 294–302 (2023).
14. O'Donnell, K. L. et al. Vaccine platform comparison: protective efficacy against lethal Marburg virus challenge in the hamster model. *Int. J. Mol. Sci.* **25**, 8516 (2024).
15. Flaxman, A. et al. Potent immunogenicity and protective efficacy of a multi-pathogen vaccination targeting Ebola, Sudan, Marburg and Lassa viruse. *PLoS Pathog.* **20**, e1012262 (2024).
16. Milligan, I. D. et al. Safety and immunogenicity of novel adenovirus type 26- and modified vaccinia Ankara-Vectored Ebola vaccines: a randomized clinical trial. *JAMA* **315**, 1610–1623 (2016).
17. Pollard, A. J. et al. Safety and immunogenicity of a two-dose heterologous Ad26.ZEBOV and MVA-BN-Filo Ebola vaccine regimen in adults in Europe (EBOVAC2): a randomised, observer-blind, participant-blind, placebo-controlled, phase 2 trial. *Lancet Infect. Dis.* **21**, 493–506 (2020).
18. Sarwar, U. N. et al. Safety and immunogenicity of DNA vaccines encoding Ebolavirus and Marburgvirus wild-type glycoproteins in a phase I clinical trial. *J. Infect. Dis.* **211**, 549–557 (2015).
19. Meyer, M. et al. Modified mRNA-based vaccines elicit robust immune responses and protect guinea pigs from Ebola virus disease. *J. Infect. Dis.* **217**, 451–455 (2018).
20. Wolff, J. A. et al. Direct gene transfer into mouse muscle in vivo. *Science* **247**, 1465–1468 (1990).
21. Essink, B. et al. The safety and immunogenicity of two Zika virus mRNA vaccine candidates in healthy flavivirus baseline seropositive and seronegative adults: the results of two randomised, placebo-controlled, dose-ranging, phase 1 clinical trials. *Lancet Infect. Dis.* **23**, 621–633 (2023).
22. Aliprantis, A. O. et al. A phase 1, randomized, placebo-controlled study to evaluate the safety and immunogenicity of an mRNA-based RSV prefusion F protein vaccine in healthy younger and older adults. *Hum. Vaccin Immunother.* **17**, 1248–1261 (2021).
23. Lee, I. T. et al. Safety and immunogenicity of a phase 1/2 randomized clinical trial of a quadrivalent, mRNA-based seasonal influenza vaccine (mRNA-1010) in healthy adults: interim analysis. *Nat. Commun.* **14**, 3631 (2023).
24. FDA US. 2021. FDA Approves First COVID-19 Vaccine. https://www.fda.gov/news-events/press-announcements/fda-approves-first-covid-19-vaccine.
25. Flyak, A. I. et al. Mechanism of human antibody-mediated neutralization of Marburg virus. *Cell* **160**, 893–903 (2015).
26. Kajihara, M. et al. Inhibition of Marburg virus budding by non-neutralizing antibodies to the envelope glycoprotein. *J. Virol.* **86**, 13467–13474 (2012).
27. Ilinykh, P. A. et al. Non-neutralizing antibodies from a Marburg infection survivor mediate protection by Fc-effector functions and by enhancing efficacy of other antibodies. *Cell Host Microbe* **27**, 976–991 e911 (2020).
28. Keck, Z. Y. et al. Macaque monoclonal antibodies targeting novel conserved epitopes within filovirus glycoprotein. *J. Virol.* **90**, 279–291 (2016).
29. King, L. B. et al. The Marburgvirus-neutralizing human monoclonal antibody MR191 targets a conserved site to block virus receptor binding. *Cell Host Microbe* **23**, 101–109 e104 (2018).
30. Richner, J. M. et al. Modified mRNA vaccines protect against Zika virus infection. *Cell* **168**, 1114–1125.e1110 (2017).
31. Mire, C. E. et al. Therapeutic treatment of Marburg and Ravn virus infection in nonhuman primates with a human monoclonal antibody. *Sci. Transl. Med.* **9**, eaai8711 (2017).
32. Hashiguchi, T. et al. Structural basis for Marburg virus neutralization by a cross-reactive human antibody. *Cell* **160**, 904–912 (2015).
33. Fusco, M. L. et al. Protective mAbs and Cross-Reactive mAbs Raised by Immunization with Engineered Marburg Virus GPs. *PLoS Pathog.* **11**, e1005016 (2015).
34. Flyak, A. I. et al. Broadly neutralizing antibodies from human survivors target a conserved site in the Ebola virus glycoprotein HR2-MPER region. *Nat. Microbiol.* **3**, 670–677 (2018).
35. Britto, C. & Alter, G. The next frontier in vaccine design: blending immune correlates of protection into rational vaccine design. *Curr. Opin. Immunol.* **78**, 102234 (2022).
36. Wong, G. et al. Development and characterization of a guinea pig model for Marburg virus. *Zool. Res.* **39**, 32–41 (2018).
37. Cross, R. W. et al. Comparison of the pathogenesis of the Angola and Ravn strains of Marburg virus in the outbred guinea pig model. *J. Infect. Dis.* **212**, S258–S270 (2015).
38. Corbett, K. S. et al. Immune correlates of protection by mRNA-1273 vaccine against SARS-CoV-2 in nonhuman primates. *Science* **373**, eabj0299 (2021).
39. Stonier, S. W. et al. Marburg virus survivor immune responses are Th1 skewed with limited neutralizing antibody responses. *J. Exp. Med.* **214**, 2563–2572 (2017).
40. Natesan, M. et al. Human Survivors of Disease Outbreaks Caused by Ebola or Marburg Virus Exhibit Cross-Reactive and Long-Lived Antibody Responses. *Clin. Vaccin. Immunol.* **23**, 717–724 (2016).
41. Peng, W. et al. Glycan shield of the ebolavirus envelope glycoprotein GP. *Commun. Biol.* **5**, 785 (2022).
42. Bale, S. et al. Structural basis for differential neutralization of ebolaviruses. *Viruses* **4**, 447–470 (2012).
43. He, W. et al. Epitope specificity plays a critical role in regulating antibody-dependent cell-mediated cytotoxicity against influenza A virus. *Proc. Natl. Acad. Sci. USA* **113**, 11931–11936 (2016).
44. Keshwara, R. et al. A recombinant rabies virus expressing the Marburg virus glycoprotein is dependent upon antibody-mediated cellular cytotoxicity for protection against Marburg virus disease in a murine model. *J. Virol.* **93**, e01865–01818 (2019).
45. Montoya, B. et al. mRNA-LNP vaccine-induced CD8(+) T cells protect mice from lethal SARS-CoV-2 infection in the absence of specific antibodies. *Mol. Ther.* **32**, 1790–1804 (2024).
46. Li, C. et al. Mechanisms of innate and adaptive immunity to the Pfizer-BioNTech BNT162b2 vaccine. *Nat. Immunol.* **23**, 543–555 (2022).

47. Laczko, D. et al. A single immunization with nucleoside-modified mRNA vaccines elicits strong cellular and humoral immune responses against SARS-CoV-2 in mice. *Immunity* **53**, 724–732.e727 (2020).
48. Orme, I. M. Mouse and guinea pig models for testing new tuberculosis vaccines. *Tuberculosis* **85**, 13–17 (2005).
49. Guo, Y. et al. Immunoglobulin genomics in the guinea pig (Cavia porcellus). *PLoS One* **7**, e39298 (2012).
50. Matsuzawa, S., Isobe, M. & Kurosawa, N. Guinea pig immunoglobulin VH and VL naive repertoire analysis. *PLoS One* **13**, e0208977 (2018).
51. Lei, L. et al. Antigen-specific single B cell sorting and monoclonal antibody cloning in guinea pigs. *Front Microbiol* **10**, 672 (2019).
52. Vukovich, M. J. et al. Development of LIBRA-seq for the guinea pig model system as a tool for the evaluation of antibody responses to multivalent HIV-1 vaccines. *J. Virol.* **98**, e0147823 (2024).
53. Hevey, M., Negley, D., Staley, A. & Schmaljohn, A. Determination of vaccine components required for protecting cynomolgus macaques against genotypically divergent isolates of Marburg virus. *20th Annual Meeting of the American Society for Virology*. **Abstract W36–4** (2001).
54. Hevey, M. et al. Marburg virus vaccines: comparing classical and new approaches. *Vaccine* **20**, 586–593 (2001).
55. Daddario-DiCaprio, K. M. et al. Cross-protection against Marburg virus strains by using a live, attenuated recombinant vaccine. *J. Virol.* **80**, 9659–9666 (2006).
56. Sahin, U., Kariko, K. & Tureci, O. mRNA-based therapeutics-developing a new class of drugs. *Nat. Rev. Drug Discov.* **13**, 759–780 (2014).
57. Towner, J. S. et al. Marburgvirus genomics and association with a large hemorrhagic fever outbreak in Angola. *J. Virol.* **80**, 6497–6516 (2006).
58. Johnson, E. D. et al. Characterization of a new Marburg virus isolated from a 1987 fatal case in Kenya. *Arch. Virol. Suppl.* **11**, 101–114 (1996).
59. Meyer, M. et al. Antibody repertoires to the same ebola vaccine antigen are differentially affected by vaccine vectors. *Cell Rep.* **24**, 1816–1829 (2018).
60. Ackerman, M. E. et al. A robust, high-throughput assay to determine the phagocytic activity of clinical antibody samples. *J. Immunol. Methods* **366**, 8–19 (2011).

Acknowledgements

We thank the UTMB Animal Resource Center for animal procedures and husbandry support. We thank Dr. Philipp A. Ilinykh for valued discussions on the findings. Figures 1, 3C, 9A were created with BioRender.com. This study was supported by a grant from National Institute of Allergy and Infectious Disease 1 R01 AI41661-01 (to A. B.).

Author contributions

M.M., S.H. and A.B. conceived the study. M.M. designed animal experiments, performed ELISAs, PRNT-based assays, BLI-based GP competition assays and peptide arrays. B.M.G. performed Fc-effector assays. C.P. and K.K. performed virus plaque assays. C.S. performed BLI-based mAb competition assays. P.P.V. performed correlation analysis and generated associated figures. M.A.H. supervised challenge studies and sampling. M.M., G.A., S.H., A.C. and A.B. supervised study. E.O.S, J.E.C, Jr. provided critical reagents. A.B. acquired funding. M.M. compiled and analyzed data, generated figures and wrote the manuscript with contributions from B.M.G., C.S. and P.P.V., and M.M., C.S., J.E.C. Jr, S.H. and A.B. edited the manuscript. All authors approved the final version of the manuscript.

Competing interests

S.H. and A.C. are employees of Moderna. J.E.C. Jr. has served as a consultant for Luna Labs USA, Merck Sharp & Dohme Corporation, Emergent Biosolutions, and BTG International Inc. and is a member of the scientific advisory board of Meissa Vaccines, a former member of the scientific advisory board of GigaGen (Grifols), and is a founder of IDBiologics. J.E.C, Jr's laboratory received unrelated sponsored research agreements from AstraZeneca, Takeda Vaccines, and IDBiologics. A.B. is a co-founder and vice-president of Emervax, Inc. The remaining authors declare no competing interests.

Additional information

Supplementary information The online version contains supplementary material available at https://doi.org/10.1038/s41467-025-60057-0.

Correspondence and requests for materials should be addressed to Andrea Carfi or Alexander Bukreyev.

Peer review information *Nature Communications* thanks James Brien and the other anonymous reviewers for their contribution to the peer review of this work. A peer review file is available.

Reprints and permissions information is available at http://www.nature.com/reprints

Publisher's note Springer Nature remains neutral with regard to jurisdictional claims in published maps and institutional affiliations.

[1]Department of Pathology, University of Texas Medical Branch, Galveston, TX, USA. [2]Galveston National Laboratory, Galveston, TX, USA. [3]Paul G. Allen School of Global Animal Health, Washington State University, Pullman, WA, USA. [4]Department of Neurobiology, University of Texas Medical Branch, Galveston, TX, USA. [5]La Jolla Institute for Immunology, La Jolla, CA, USA. [6]Department of Pathology, Microbiology, and Immunology, Vanderbilt University Medical Center, Nashville, TN, USA. [7]Department of Pediatrics, Vanderbilt University Medical Center, Nashville, TN, USA. [8]Vanderbilt Vaccine Center, Vanderbilt University Medical Center, Nashville, TN, USA. [9]Ragon Institute of MGH, MIT and Harvard, Cambridge, MA, USA. [10]Moderna Inc., Cambridge, MA, USA. [11]Department of Microbiology & Immunology, University of Texas Medical Branch, Galveston, TX, USA. [12]Center for Biodefense and Emerging Infectious Diseases, University of Texas Medical Branch, Galveston, TX, USA. ✉e-mail: andrea.carfi@modernatx.com; alexander.bukreyev@utmb.edu